Palaeontologia Electronica
palaeo-electronica.org

Amakusaichthys benammii sp. nov., a Campanian long-nose ichthyodectiform fish from the Tzimol Quarry, Chiapas, southeastern Mexico

Jesús Alvarado-Ortega

ABSTRACT

Amakusaichthys benammii sp. nov. is described based on specimens recovered from the Campanian shallow marine deposits of the Tzimol Quarry near Comitán, Chiapas, Mexico. The species fits the diagnosis of the basal teleost order Ichthyodectiformes. Moreover, the species is located in the long-nose genus *Amakusaichthys* because it has two highlight features previously documented in the Japanese species *A. goshouraensis,* including the elongation of the skull ethmoid region and the reinforcement of the caudal skeleton. The specimens of the new species are preserved in 3D, revealing some outstanding osteological features that support its uniqueness and the amendment of the generic diagnosis; the ethmoid skull region is elongated, causing the long-nose appearance of this fish and the anterior displacement of its ethmopalatine upper jaw articulation away from the orbit. This new Mexican species exhibits numerous distinctive features, including a strongly ornamented skull with multiple pores and short ridges; the presence of two masticatory-like plates at the end of parasphenoid ventral processes, the anterior is a heart-shaped plate and the posterior one is arrow-shaped; the hypural 3 is notably shorter than hypural 2; and the maxilla shows a palatine notch. Comparative and phylogenetic analysis indicates that *A. benammii* is closely related to *A. goshouraensis* and the genus *Heckelichthys*; therefore, these are grouped into the new family Heckelichthyidae. The same comparative essay also suggests that after the critical reviews, *Altamuraichthys* and *Garganoichthys* may be part of this family.

Jesús Alvarado-Ortega. Instituto de Geología, Universidad Nacional Autónoma de México, Ciudad Universitaria, Colonia Copilco, Alcandía Coyoacán, Ciudad de México, 04510 México.
alvarado@geología.unam.mx

Keywords: Icthyodectiformes; *Amakusaichthys;* Campanian; Tzimol; Chiapas; Mexico

https://zoobank.org/DB76EBA3-1850-43B7-A345-CADC23836CC1

Final citation: Alvarado-Ortega, Jesús. 2024. *Amakusaichthys benammii* sp. nov., a Campanian long-nose ichthyodectiform fish from the Tzimol Quarry, Chiapas, southeastern Mexico. Palaeontologia Electronica, 27(3):a59.
https://doi.org/10.26879/1444
palaeo-electronica.org/content/2024/5295-a-long-nose-ichthyodectiform

Submission: 29 August 2024. Acceptance: 12 December 2024.

INTRODUCTION

Ichthyodectiformes is a worldwide Mesozoic clade of primitive teleost fishes, including *Ichthyodectes* Cope, 1870, and relatives (Bardack and Sprinkle, 1969). The first member of this group known, initially confused as a reptile, was described 200 years ago as *Saurocephalus lanciformis* Harlan, 1824. A century and a half later, Bardack and Sprinkle (1969) recognized the monophyly of these fishes and erected the order Ichthyodectiformes, diagnosed today with a series of peculiar features (e.g., Maisey, 1991; Cavin et al., 2013). Although some Asian species from the Early Cretaceous (which belonging to this order is questioned in the present work) are from freshwater deposits (Kim et al., 2014), fossils of other ichthyodectiforms came from epicontinental marine deposits from the Middle Jurassic (Bathonian) to the Late Cretaceous (Maastrichtian) (Patterson and Rosen, 1977; Schaeffer and Patterson, 1984).

Amakusaichthys goshouraensis Yabumoto, Hirose, and Brito, 2018, is a peculiar Japanese ichthyodectiform discovered in the Santonian section of the Hinoshima Formation (Himenoura Group) at Maeshima islet of Goshoura Island, Amakusa City, in the Kumamoto Prefecture. This species has a peculiar caudal skeleton reinforcement that consists of the proximal elongation of the rays that form both caudal lobes plus the development of a prominent dorsal ridge in the hypural 2 that is bent laterally and forms a triangular structure resembling the folded corner of a blanket on the bed. The present work aims to describe a new species of *Amakusaichthys* based on well-preserved Campanian specimens from the Tzimol Quarry, a paleontological site in Chiapas, Mexico. This report of *Amakusaichthys* is the second worldwide and the first in America.

The known Mexican ichthyodectiform fossils are from different Kimmeridgian–Campanian deposits of shallow marine environments, which, during the Late Jurassic and Cretaceous, represented the western realm of the Paleogulf of Mexico. These sites belong to the states of Chiapas (the El Chango and Tzimol quarries), Coahuila (multiple sites around Múzquiz), Guerrero (Arroyo Las Bocas Quarry), Hidalgo (Muhi Quarry), Nuevo León (Vallecillo Quarry), Puebla (Tlayúa and San José de Gracia quarries), San Luis Potosí (Xilitla Quarry), and Zacatecas (Mazapil beds). Cope (1871) described the first Mexican ichthyodectiform in the second half of the nineteenth century; however, the scientific studies on these fishes and, in general, the development of Mexican paleoichthyology were inadequate for a 100 years more. Such a scenario changed in the 1980s with the discovery of the Tlayúa Quarry and the subsequent development of young national researchers (Alvarado-Ortega, 1998, 2005; Alvarado-Ortega et al., 2006a, 2006b). Thus, the earliest of these reports (Cope, 1871; Felix, 1891; Maldonado-Koerdell, 1956) are of little interest because these involved scarce and non-diagnosable skeletal remains or paleontological sites undescribed. Despite this, today, the Mexican diversity of ichthyodectiforms includes the species *Xiphactinus audax* Leidy, 1870; *Prymnetes longiventer*, Cope, 1871; *Gillicus arcuatus* Cope, 1875; *Vallecillichthys multivertebratum* Blanco and Cavin, 2003; *Unamichthys espinosai* Alvarado-Ortega, 2004; and *Heckelichthys preopercularis* Baños-Rodríguez, González-Rodríguez, Wilson, and González-Martínez, 2020. Among Mexican fossils, indeterminate species belonging to different genera have also been reported, as *Saurodon* Hays, 1830; *Thrissops* Agassiz, 1833; and *Heckelichthy* Taverne, 2008; as well as possible new ichthyodectiforms present in the Tlayúa and Tzimol quarries (e.g., Alvarado-Ortega et al., 2006a, 2006c, 2009, 2020; Villaseñor et al., 2006; Blanco-Piñón and Alvarado-Ortega, 2007; Alvarado-Ortega and Porras-Múzquiz, 2009, 2022; González-Rodríguez et al., 2013; Baños-Rodríguez, 2018).

The Tzimol Quarry is a paleontological site near Comitán Municipality, Chiapas, southeastern Mexico (Alvarado-Ortega et al., 2019, 2020), extending between the coordinates 16°12′57.52″–16°13′49.22″ N and 92°15′00″–92°16′11″ W, close to the western edge of the Upland Central Region of Chiapas (Figure 1). This Fossil-Lagerstätte consists of interconnected small quarries opened outside the Ochuxhob town (also called Ochusjob and Ochuxhjob), in which the local people extract parallel centimetric-decimetric marl strata flagstones that interbed some thin clay layers. Such sequence forms part of the Campanian shallow and restricted marine deposits of the Angostura Formation, previously named by Sánchez-Montes de Oca (1979). Up to now, the Tzimol fossil assemblage includes microfossils, as foraminifers, ostracods, and algae

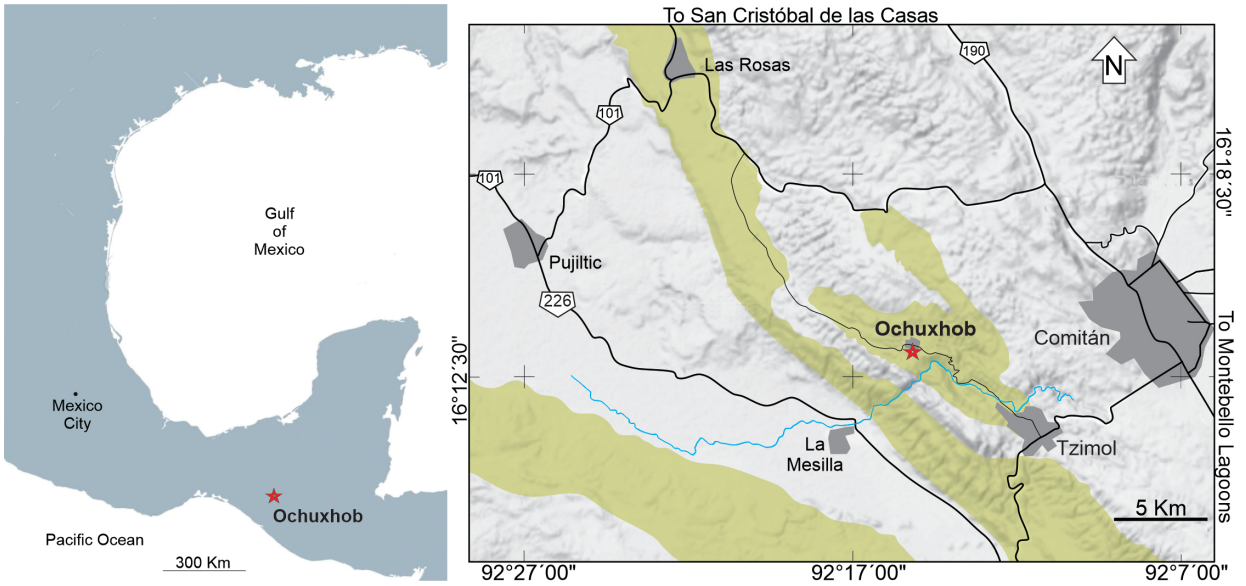

FIGURE 1. Map of the Tzimol–Comitán region showing the outcrops of the Angostura Formation (in green color) exploited at the Tzimol Quarry (red star), outside of the Ochuxhob town, Tzimol Municipality, Chiapas, southeastern (Based on Alvarado-Ortega et al., 2020, figure 1).

(Lupercio Espericueta, 2022), as well as macrofossils of plants (remains include leaves, flowers, and possible fruits), invertebrates (including the Campanian index fossil *Radiolites acutocostata* (Adkins, 1930), trigonid bivalve, spatangoid echinoids, gastropods, and scaphopods), and vertebrates that involve scarce mosasaur remains and abundant fishes that include indeterminate Acanthomorpha (Carranza-Becerra et al., 2023), *Nursallia* Blot, 1987 (Pycnodontiformes); *Saurodon* Hays, 1830 (Ichthyodectiformes); *Enchodus* Agassiz, 1833 (Enchodontidae); as well as the species *Apuliadercetis gonzalezae* Díaz-Cruz, Alvarado-Ortega, Cantalice, 2022 (Dercetidae) and *Macabi tojolabalensis* L-Recinos, Cantalice, Caballero-Viñas, and Alvarado-Ortega, 2023 (Albuliformes).

MATERIAL AND METHODS

Preparation Methods

Preparing the specimens studied here followed the mechanical and chemical procedures of Toombs and Rixon (1959). Under a stereoscopic microscope, needles, dental excavators, and fine air scribes helped to mechanically remove the small rock matrix from the surfaces of fossil structures. The acid-cleaning technique allowed the elimination of the marly matrix because of the reaction with its calcareous component. The immersion in acetic acid solution and clean water applied to specimens transferred and non-transferred was repeated as many times as necessary until the fossil structures were exposed or their physical integrity reached a high-risk point. The bones fractured or loose during the preparation are glued with cyanoacrylate. Additionally, once the preparation of the specimens was considered complete, the surfaces of the fossils were hardened with a weak solution of plexigum PQ 611 diluted in methacrylate acetate applied with a fine brush.

The specimens were observed with the naked eye, under stereo microscopy, and through high-resolution photographs obtained under different conditions in a photographic laboratory with the specimens uncoated and coated with magnesium smoke. These conditions include controlling the intensity and incidence angle of the illumination and using diverse light sources, including natural, white, and long-wave UV (254 nm) light. The CorelDraw Graphics Suite 2021 program made it possible to colorize and highlight the shape of some bones in the photos illustrating this work.

Institutional Abbreviations

The fossils studied here are deposited and cataloged under the acronym IGM, which corresponds to the Colección Nacional de Paleontología, housed in the Instituto de Geología of the Universidad Nacional Autónoma de México. Other fossils studied here belong to the following institutions: AMNH, American Museum of Natural History, New York, USA; DNPM, Departamento Nacional de Produção Mineral, Rio de Janeiro, Brazil; MUZ, Museo de Paleontología de Múzquiz,

Coahuila, Mexico; USNM, United States National Museum, Washington, USA; UERJ-PMB, Paleontological Collection of the Universidade do Estado do Rio de Janeiro, Brazil, under the care of Dr. Paulo Marques Brito.

Comparative Materials

The specimens studied here with comparative proposes include the following species. *Chiromystus alagoensis* Jordan, 1910, AMNH 10015, ANMH 10016, impression and silicon casts of nearly complete specimens from Early Cretaceous, Riacho Doce, Alagôas, Brazil. *Cladocyclus gardneri* Agassiz, 1841: AMNH 10015 and AMNH 10016, both from Riacho Doce, Alagoas, Brazil. *Cladocyclus* sp.: AMNH 3875, AMNH 11868, AMNH 11877, AMNH 19129, all from the Santana Formation, Ceará, Brazil. *Gillicus arcuatus* (Cope, 1875): AMNH 8571, from the Niobrara Formation, Kansas, USA, and MUZ 47, from the El Pilote Ranch, Coahuila, Mexico. *Ogunichthys triangularis* Alvarado-Ortega and Brito, 2010: holotype UERJ-PMB 100 and referred specimens UERJ-PMB 93, 94, 95, 97, 98, 99 and DNPM 533-P, 534-P, and 544-P; all from the Marizal Formation (Tucano Basin), Bahía, Brazil. *Prymnetes longiventer* Cope, 1871: silicon cast deposited in IGM the specimen USNM 4090, from an unknown site near Tuxtla Gutiérrez, Chiapas, Mexico. *Saurodon leanus* Hays, 1830: AMNH 9907 from the Niobrara Formation, Kansas, USA; IGM 676, from La Mula Quarry, Coahuila, Mexico. *Unamichthys espinosai* Alvarado-Ortega, 2004: IGM 8373-IGM 8376 (type series), from the Tlayúa Quarry, Puebla, Mexico. *Xiphactinus audax* Leidy, 1870: AMNH 1973, AMNH 7350, AMNH 8547, AMNH 8574, AMNH 1639, and AMNH 19528, all from the Niobrara Formation, Kansas, USA; and MUZ-3912 from the Austin Group outcrops in the Piedritas site, Coahuila.

Anatomical Terminology and Abbreviations

The anatomical terminology and abbreviations used in this contribution are like those of previous publications dealing with the anatomy of the Ichthyodectiformes (e.g., Bardack, 1965; Patterson and Rosen, 1977; Cavin et al., 2013; Yabumoto et al., 2018).

Phylogenetic Analysis

The relationships of the species described here resulted from a phylogenetic analysis based on the study B performed by Hacker and Shimada (2021), which at the same time is constructed with data from previous studies (Cavin et al., 2013; Yabumoto et al., 2018; Cavin and Berrell, 2019; Baños-Rodríguez et al., 2020).

The data matrix of this work involves 77 osteological characters [72 of Hacker and Shimada (2021, appendices 3–4)] and 33 taxa (see Tables S1–S2 in Appendix 1). This data matrix is captured in the program Mesquite Version 3.81 (Maddison and Maddison, 2023) (Appendix 2). It adds data on the species described here, five new characters, and characters of *Amakusaichthys goshouraensis* reinterpreted from the main text and figures of Yabumoto et al. (2018).

This research evaluates the interrelationships of the new Mexican species of *Amakusaichthys* based on the results of two phylogenetic analyses (see Table S3 in Appendix 1). The first includes all the species considered by Baños-Rodríguez et al. (2020), plus the new Mexican species, while the second excludes *Bardackichthys carteri* Hacker, Shimada, 2021; *Jinjuichthys cheongi* Kim, Chang, Wu, and Kim, 2014; and *Mesoclupea showchangensis* Ping, Yen, 1933, because these species have some morphological attributes suggesting that they do not belong to the order Ichthyodectiformes. The execution of both analyses follows the heuristic search protocol performed with the program PAUP Version 4.0a (Swofford, 2002). All characters were unweighted and unordered. Question marks (?) and hyphens (-) represent the missing and inapplicable data. This analysis has *Elops hawaiensis* Regan, 1909 as the outgroup. This protocol consists of the random addition sequences with 1000 replicates and 10 trees held at each iteration, as well as the tree bisection and reconnection branch swapping. The assessment of the resulting phylogenetic hypothesis includes two tests: the Bremer branch support values calculated using the converse constraint option of PAUP, and the Bootstrap branch stability results from 1000 replicas using the random additional algorithm under a simple search protocol.

SYSTEMATIC PALEONTOLOGY

Subdivision TELEOSTEI Müller, 1844
Order ICHTHYODECTIFORMES Bardack and Sprinkle, 1969
Suborder ICHTHYODECTOIDEI Romer, 1966
Family HECKELICHTHYIDAE fam. nov.

zoobank.org/78FDECF6-A944-47C3-9BB7-B632E74C2587

Included genera. *Heckelichthys* Taverne, 2008. *Amakusaichthys* Yabumoto, Hirose, and Brito,

2018. And probably *Garganoichthys* Taverne, 2009, and *Altamuraichthys* Taverne, 2016.

Diagnosis. Ichthyodectoidei fishes with the supraoccipital crest large, shallow, and do not project beyond the base of the skull; teeth in both jaws are evenly small or absent; preopercle with a long horizontal limb; mandibular articulation below and in front of the orbit; pelvic fin located in the posterior third of the standard length, close to the anal fin origin; the origins of the unpaired fins opposed to each other; and the caudal fin has with a ventral lobe at least 1.5 times longer than the dorsal lobe.

Genus *AMAKUSAICHTHYS*
Yabumoto, Hirose, and Brito, 2018

Included species. *Amakusaichthys goshouraensis* Yabumoto, Hirose, and Brito, 2018. *Amakusaichthys benammii* sp. nov. described below.

Emended diagnosis. Ichthyodectiform fish with an extended ethmoid region of the skull; small mouth; supraoccipital crest shallow and short; parietals medially fused; lower jaw-quadrate articulation located ahead of the orbit; maxilla comparatively short and sinuous; lower jaw rectangular and relatively short; jaw teeth small, conical, and evenly sized and spaced; ethmopalatine bone long and far from the nasal capsule, with osseous membranous suturing projections and ventral articular facets located below the rostrodermethmoid bone; palatine head high, disk-like malleolus, and with a ventral expanded wing; preopercle with a long ventral limb and the posterior edge intensely fringed; preopercular sensory canal with numerous curved parallel branches in the preopercle horizontal limb; pelvic fin placed very close to the origin of the anal fin; unpaired fins located far in the back of the trunk, including a dorsal fin placed slightly ahead of the long anal fin; rays of the caudal dorsal and ventral lobes anteriorly extended, covering most of the caudal skeleton; neural arches of the most posterior preural centra have dorsoanterior saddle-shaped processes supporting the adjacent anterior neural spine; hypural 1 spatuliform; hypural 2 large and triangular with a prominent dorsal ridge bent laterally, forming a triangular structure resembling the folded corner of a blanket on the bed that is pierced by three large pores; articular heads of hypurals 1–2 and parahypural broad an in lateral contact; hypural 3 slightly shorter than hypural 2; trunk entirely covered with large thin cycloid scales ornamented with numerous concentric circulii, central puntae, and scarce anterior and parallel radii.

Amakusaichthys benammii sp. nov.

zoobank.org/F7C9689F-D7D1-4182-95D9-23EDE83E74DE

Holotype. IGM 14027, a nearly complete specimen preserved in part (IGM 14027a) and counterpart (IGM 14027b), both transferred to resin (Figure 2).

Paratypes. IGM 14028, a complete and articulated specimen preserved in part (IGM 14028a) and counterpart (IGM 14028b). IGM 14029, an incomplete specimen with the head dorsally titled and lacking the caudal part. IGM 14030, an incomplete specimen without the post pelvic part of the trunk, preserved in part (IGM 14030a) and counterpart (IGM 14030b), both transferred to resin. IGM 14031, head and part of the abdominal region with bones somewhat scattered. IGM 14032, head fish with both limbs of the lower jaw disarticulated. IGM 14033, head lacking the ethmoid anterior tip, preserved in part (IGM 14033a) and counterpart (IGM 14033b). IGM 14034, a vertebral column nearly complete, transferred to resin. IGM 14035, a fragment of the posterior part of the trunk with the caudal skeleton. IGM14036, head and part of the abdominal region.

Etymology. The species epithet honors my friend and colleague, Dr. Mouloud Benammi, for his valuable contributions to Mexican paleontology and paleomagnetostratigraphy (Figure 3).

Age and distribution. All specimens come from the Campanian marly deposits of the Angostura Formation extracted in the Tzimol Quarry outside the Ochuxhob town, Comitán Municipality, Chiapas, southeastern Mexico.

Diagnosis. Compared to its sister species *Amakusaichthys goshouraensis, A. benammii* is distinguished by the skull strongly ornamented with numerous pores plus sinuous and short ridges, mainly present on the frontal and parietal bones (in *A. goshouraensis* the skull is relatively smooth); small frontal-parietal fontanel (unknown in *A. goshouraensis*); two masticatory-like processes present in the parasphenoid bones behind the basipterygoid process (unknown in *A. goshouraensis*); ethmopalatine with a dorsal extension bordering the nasal capsule dorsoanteriorly (*A. goshouraensis* lacks such ethmopalatine dorsal extension); the maxilla has a dorsal small palatine notch (*A. goshouraensis* lacks this maxillary palatine notch); the hypural 2 is 1.5 times longer than hypural 3 (the hypural 3 only marginally shorter than the hypural 2 in *A. goshouraensis*); the hypural 3 with a small folded corner ridge similar to that of the hypural 2 but projected ventrodorsally and

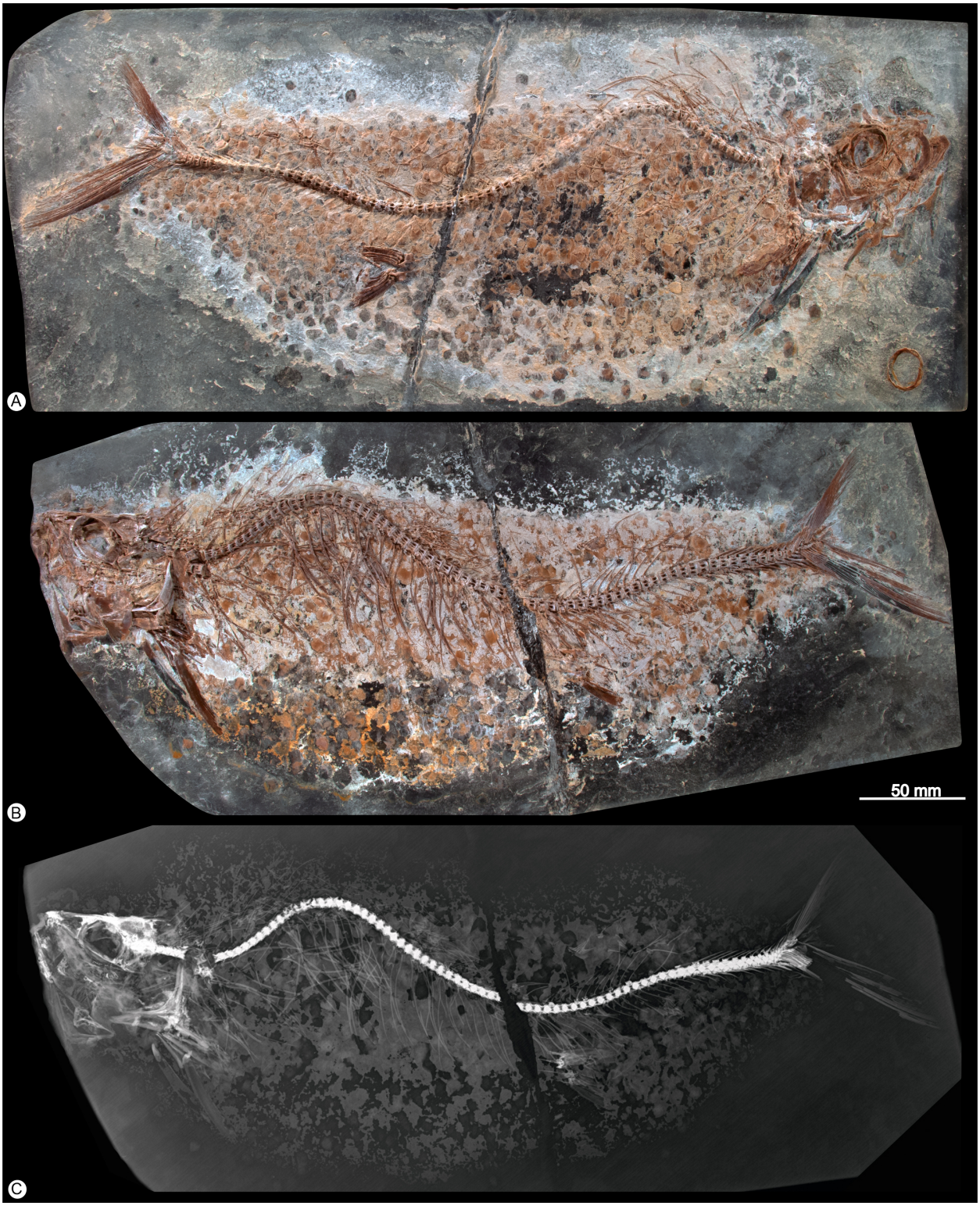

FIGURE 2. IGM 14027, holotype of *Amakusaichthys benammii* sp. nov. from the Tzimol Quarry, Chiapas, Mexico. **A,** part (IGM 14027a) of the specimen transferred to resin and observed under white light. **B,** the counterpart of the specimen (IGM 14027b) transferred to resin and observed under white light. **C,** X-ray image of IGM 14027b.

FIGURE 3. Dr. Mouloud Benammi (summer, 2024), Moroccan paleomagnestostratigrapher, to whom the specimen described in this manuscript is dedicated.

unpierced (in *A. goshouraensis*) this ridge is unknown); the vertebral column has 78 total centra including 54 abdominals, 22 preurals, and two urals (*A. goshouraensis* has nearly 76 total centra but among these 50 are abdominals, 24 preurals, and two urals).

Description

General features and proportions. Table 1 summarizes the measurements and body proportions of the specimens described here as *Amakusaichthys benammii* sp. nov. In this elongated-bodied fish, the length and height of the triangular head represent 18.5 and 13.2% of the SL, respectively. The trunk is evenly high along its predorsal region, which is barely higher than the head and represents 14% of the SL; behind, the trunk becomes less high up to the caudal peduncle, whose height only represents 5.2% of the SL. The short mouth

TABLE 1. Measurements, body proportions, and meristic data of the *Amakusaichthys benammii* sp. nov. specimens. All measurements are in millimeters. The proportions correspond to the % of the LS; "–" shows unavailable data.

Measurement	IGM 14027	IGM 14028	IGM 14029	IGM 14030	IGM 14031	IGM 14032	IGM 14034	Means or modes
Total length (TL)	454	473	–	–	–	–	–	–
Standard length (SL)	391	385	310+	–	215+	–	–	388
Head length (HL)	70	72	67	–	72	89	–	74.2
HL as % of SL	17.9	18.7	–	–	–	–		18.2
Head height (HH)	52	51	50	–	57?	62?	–	51
HH as % of SL	13.3	13.2	–	–	–	–		13.2
Maximum body height (MBH)	54	55	52?	–	–	–	–	54.5
MBH as % of SL	13.8	14.2	–	–	–	–		14
Prepelvic length (PPL)	274	270	227?	–	180?	–	–	272
PPL as % of SL	70	70	–	–		–		70
Predorsal length (PDL)	?	310	–	–	–	–	–	310
HL as % of SL	(–)	80.5	–	–	–	–		80.5
Dorsal fin length (DFL)	–	21	–	–	–	–	–	21
DFL as % of SL	–	5.4	–	–	–	–		5.4
Preanal length (PAL)	323	319	–	–	–	–	–	314
PAL as % of SL	(82.6)	81	–	–	–	–		81
Anal fin length (AFL)	24?	35	–	–	–	–	–	31
AFL as % of SL	(6.1)	9		–	–	–		9
Caudal peduncle height (CPH)	21	20	–	–	–	–	–	20.2
CPH as % of SL	(5.3)	5.1	–	–	–	–	–	5.2
Total vertebrae	78	78	65+	58+	42+	–	73+	78
Abdominal vertebrae	54	54	–	–	–	–	54?	54
Caudal vertebrae	22	22	–	–	–	–	19?	22
Pectoral fin rays	12	12	12	11?	12	12	–	12
Pelvic fin rays	8	8	7+	–	6+	–	–	8
Dorsal fin rays	4+	13	–	–	–	–	–	13
Anal rays	6+	11	–	–	–	–	–	11

opens upward; the lower jaw articulates the skull below and ahead of the orbit. The paired fins are near the trunk borders. The dorsal and anal fins rise into the last fifth of the SL. The dorsal fin is short and spreads between 80.5 and 85.9% of the SL; on the contrary, the anal fin is slightly longer and extends between 81 and 90% of the SL. The pelvic fin is placed in the posterior half of the abdomen, at 70% of the SL, about 4.5 times farther from the pectoral fin than from the anal fin. The caudal fin is deeply forked and consists of two triangular opposed and noticeably uneven-sized lobes, with the ventral lobe nearly two times longer than the dorsal one.

Skull. In lateral view, the skull is roughly triangular, tapered, and rounded anteriorly (Figures 2, 4, 5). From the anterior tip of the ethmoid region to the occipital condyle, it is nearly 1.6 times longer than high. The postorbital region is relatively small and hardly represents 25% of the skull length; in contrast, the orbit and the ethmoid region occupy the rest of the skull almost equally, with the orbit only slightly larger. The anterior projection of the principal axis of the hyomandibular fossa is anteroventrally oblique to the orbital section of the parasphenoid bone and passes below the skull ethmoid region. The inflection angle of the parasphenoid is between 120 and 135° (see below).

The skull is triangular in dorsal and ventral views (Figures 4–6). Its ethmoid region is triangular, almost 1.5 times longer than it is wide, and tapered and rounded anteriorly. In contrast, its post-ethmoid region is rectangular, barely 1.3 times longer than wide, and has sinuous lateral edges in which the frontals (= parietal sensu Schultze, 2008) have a long and shallow concave curvature above the orbital. Behind the orbital, the roof of the skull is pierced medially by a small frontal-parietal fontanel.

The rostrodermethmoid is a complex bone dorsally extended in the anterior quarter of the skull length (Figures 5–6). This triangular bone is not constrained laterally in the dorsal view. In the dorsal view, this broad triangular bone covers most of the ethmoid region and a large part of the olfactory cavity. This bone has numerous zigzagging sutures that attach its entire posterior edge to both frontals. Three small processes are present in the anterior part of this bone; a narrow and rounded anterior medial process forms the skull tip, and two small lateral descending processes suture the ethmopalatine bones. The supraethmoid is almost entirely covered by the rostrodermethmoid, except for two small regions: one exposed below the junction between the rostrodermethmoid and mesethmoid in the anterior inner region of the nasal capsule in IGM 14027; the other forming part of the crescent maxillary facet of the ethmoid region (Figure 5). In its anterior tip and between its lateral processes, the rostrodermethmoid is superficially smooth; however, further back, it is intensely ornamented by numerous pores and sinuous ridges of irregular size and arranged in a radiant pattern from the tip of the bone (Figures 5–6).

The ethmopalatine is a paired elongated complex bone in the ventral part of the skull ethmoid region that borders the nasal capsule and laterally has three processes that contact the frontal, supraethmoid, rosterodermethmoid and lateroethmoid bones (Figures 5–6). In lateral view, the posterior limb of this bone sutures in a deep zigzagging pattern with the anterior descendent process of the lateroethmoid bone. The dorsal limb of the ethmopalatine forms the anterior and dorsal edges of the nasal capsule below the respective frontal bone. It reaches the level of the ascending limb of the lateroethmoid. The anterior ethmopalatine limb precedes a deep ventral notch, showing an irregular surface and outgrowths suturing with the lateral descending process of the rostrodermethmoid. The anterior ethmopalatine limb forms part of two ventral facets, lying ahead and close to the anterior end of this part of the head, far from the nasal capsule. The anterior of these facets articulates the most anterior dorsal maxillary process and is formed by the ethmopalatine and the supraethmoid; in contrast, the posterior facet is formed only by the ethmopalatine and joints with the head of the palatine. The ethmopalatine is smooth except for part of its dorsal limb, which shows the same pattern of pores and ridges in the posterior part of the rostrodermethmoid and frontal.

The lateroethmoid consists of a triradiate wing laterally exposed plus a thin medial concave wing forming the anterior wall of the orbit (Figures 5–6). The posterodorsal limb of this bone is broad, forms its anterior third, sutures the frontals, and borders the posterior nasal capsule posteriorly. The posteroventral limb of this bone extends ventrally beyond the parasphenoid. The anterior process is as long as the nasal capsule and sutures the ethmopalatine bone, following a deep zigzagging pattern. The foramen for the olfactory nerve is exposed in a laminar and rounded medial component of this bone extended into the nasal capsule. In IGM 14027, the nasal bone is an elongated rod-like structure preserved in the nasal capsule. In the base of the skull ethmoid region, the vomer is an

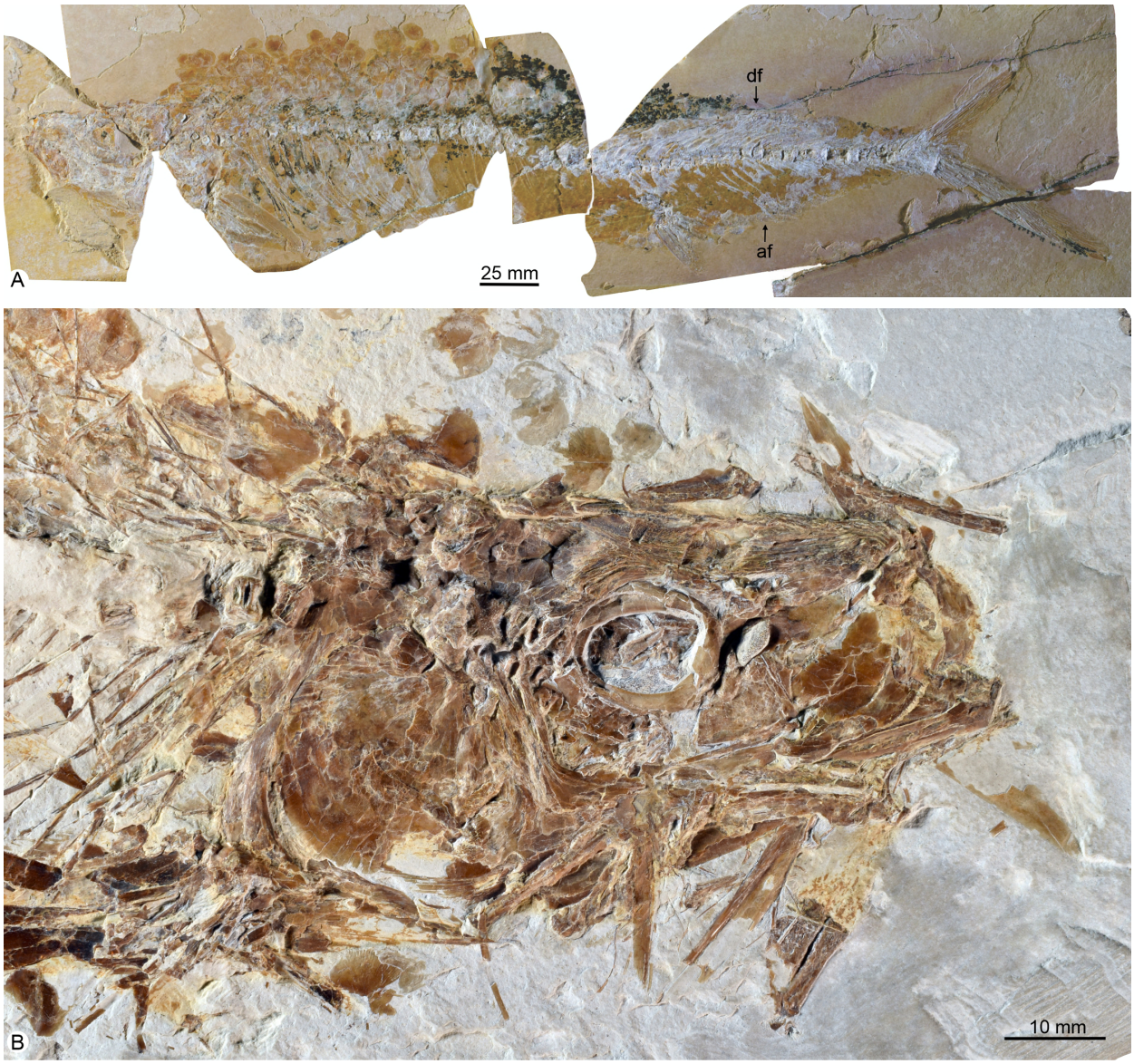

FIGURE 4. Some paratypes of *Amakusaichthys benammii* sp. nov. from the Tzimol Quarry, Chiapas, Mexico. **A,** IGM 14028a, a complete specimen. **B,** IGM 14029, close-up of the head.
Abbreviations: af, anal fin (origin); df, dorsal fin (origin).

elongated toothless bone with a broad anterior expansion and a long and sharp posterior limb that sutures with the parasphenoid.

The frontals are roughly rectangular bones that cover a little less than half the length of the skull above the orbit. These are anteriorly broad, posteriorly expanded, and joined together by a slightly sinuous middle suture that extends along their entire length except at the most posterior end, where these separate to form the anterior third of the frontal-parietal fontanel. The posterior end of each frontal sutures to the mesoparietal, pterotic, and sphenotic posteriorly while anteriorly attaching to the rostrodermethmoid and lateroethmoid. The lateral edge of the frontal that roofs the nasal capsule is straight, not notched (Figures 5–7). Numerous pits and ridges showing two patterns cover the dorsal surfaces of the frontals: 1) around the middle suture, these bones exhibit an oval zone in which these ornaments radiate from the point furthest from the side edges; 2) around this oval zone, such ornaments are posteroanteriorly aligned.

The parietals (= postparietal sensu Schultze, 2008) are fused, forming a single mesoparietal (Figures 5–6). This huge bone is far from the posterior skull edge, roofs nearly half of the skull

FIGURE 5. Close-up of the left side of the skull of IGM 14027b, counterpart of the holotype of *Amakusaichthys benammii* sp. nov. transferred to resin and coated with magnesium.
Abbreviations: boc, basioccipital; bptp, basipterygoid process; bsc, basal sclerotic bone; bsp, basisphenoid; ect, ectopterygoid; epi, epioccipital; etpa, ethmopalatine; exo, exoccipital;exsc, extrascapular; fpf, frontoparietal fontanel; fr, frontal; int, intercalar; let, lateroethmoid; mlp, masticatory-like processes in the parasphenoid bone; mp, mesoparietal (=parietals fused); ors, orbitosphenoid; pas, parasphenoid; pto, pterotic; pts, pteroshpenoid; rode, rostrodermethmoid; soc, supraoccipital; sop, subopercle; sph, sphenotic; stt, supratemporal; suo, supraorbital.

behind the orbit, and sutures the frontal, pterotic, supraoccipital, and epioccipital. Although this bone has a slight medial elevation before suturing to the anterior tip of the supraoccipital, it definitively does not form part of the supraoccipital crest. Posteriorly, the mesoparietal has two posterior lateral projections that barely border the anterior end of such crest. Also, the mesoparietal borders the posterior two-thirds of the narrow frontal-parietal fontanel. Numerous pits of irregular size and random distribution in the mesoparietal surface.

The posterior half of the dorsal postorbital region of the skull is occupied chiefly by three elongated bones that form conspicuous crests (Figures 5–6). In the middle, the supraoccipital displays a thin and triangular supraoccipital crest with a concave posterior border, culminating in an acute dorsoposterior tip that projects up to the level of the occipital condyle. In a lateral position to this medial crest, the epioccipital bones rise, forming a couple of relatively shallow robust epioccipital crests that are straight and project posteriorly up to the base of the posterior border of the supraoccipital crest. These bones are smooth superficially.

The autosphenotic is a triangular bone that borders the posterodorsal part of the orbit and sutures the frontal dorsally and the pterotic posteriorly (Figures 5–6). A medial extension of this bone behind the orbit forms part of the anterior end of the hyomandibular fossa. The ventral opening of the supraorbital canal is so large and deep in this bone that it separates the superficial plane of this bone, giving it an inverted Y appearance.

The pterotic is a somewhat trapezoidal bone exposed in the dorsolateral surface of the skull postorbital region (Figures 5–6). This bone joins the intercalar ventroposteriorly, the autosphenotic ventroanteriorly, and the frontal, parietal, and epioccipital medially. The anterior tip of this bone sutures the frontal ahead of the autosphenotic.

FIGURE 6. Close-up of the skull of IGM 14030, paratype of *Amakusaichthys benammii* sp. nov. preserved in part and counterpart transferred to resin and coated with magnesium. **A,** dorsal view of the skull in IGM 14030a. **B,** Ventral view of the skull in IGM 14030b.
Abbreviations: boc, basioccipital; bptp, basipterygoid process; bsh, basisphenoid; ect, ectopterygoid; epi, epioccipital; etpa, ethmopalatine; exo, exoccipital; exsc, extrascapular; fpf, frontoparietal fontanel; fr, frontal; int, intercalar; let, lateroethmoid; mlp, masticatory-like processes in the parasphenoid bone; mp, mesoparietal (=parietals fused); ors, orbitosphenoid; pas, parasphenoid; pro, prootic; pto, pterotic; pts, pteroshpenoid; rode, rostrodermethmoid; soc, supraoccipital; sop, subopercle; sph, sphenotic; suet, supraethmoid; suo, supraorbital; vo, vomer; (l), paired bone of the left side; (r), paired bone of the right side.

Posteriorly, it joins the exoccipital bone and roofs the posttemporal fossa. Additionally, it forms part of the posterior edge of the skull, shows an anterodorsally inclined fold that forms the roof of the lateral temporal fossa, and its ventral border covers the temporal region of the skull that houses the hyomandibular and supratemporal fossae. The pterotic has a deep groove in which the otic sensory canal opens. Numerous pits aligned radially from its center cover the surface of this bone.

The intercalar bone is elongated and occupies the posterolateral part of the postorbital region of the skull, suturing the basioccipital ventrally, the protic anteriorly, and the pterotic dorsally (Figures 5–6). The ventral part of this bone becomes a noticeable lateral protruding massive structure behind the orbit. This massive bone extends forward, forming the posterior end of the hyomandibular fossa and ventrally roofs the jugal canal (where the jugular vein runs and the foramina for the glossopharyngeal and vagus nerves open).

The bones of the ventral part of the skull are exposed laterally in IGM 14027 and ventrally in IGM 14030 (Figures 5–6). The prootic is a broad rectangular bone occupying most of the skull postorbital region behind the orbit. Dorsally, the prootic forms the large and middle part of the hyomandibular fossa and forms most of the subtemporal fossa. Near its dorsoanterior end, the prootic has two large foramina corresponding to the hyomandibular and palatine branches of the cranial nerve VII. The basioccipital bone forms the basal half of the skull's posterior height. This bone is rectangular in both views and shows deep depressions around the occipital condyle. The sharp and deeply zigzagging projections of the parasphenoid extend almost along the entire length of the basioccipital, providing a tight suture between them. The occipital condyle is an articular surface formed only by the basioccipital, in which its rounded shape has a deep concave cavity.

The parasphenoid is an elongated complex and toothless bone with two differentiable parts (Figures 5–6). Anteriorly, the orbital parasphenoid section is a long bar extended along the orbit and most of the base of the ethmoid region below the vomer. This parasphenoid section is inverted T-shaped in cross section and consists of a high dorsal lamina plus a ventral horizontal lamina expanded in its anterior and posterior ends. In ventral view, this horizontal lamina has a deep anterior notch to allocate the posterior limb of the vomer; in contrast, its posterior end expands laterally and forms a T-shaped structure together with the pair of basipterygoid processes that are long, straight, and tilted laterally, ventrally, and anteriorly. The postorbital parasphenoid expands dorsally to form the basal lateral quarter of the skull. It has an elongated sharp posterior projection to suture the basioccipital bone, almost reaching the occipital condyle. Behind and below the basipterygoid process, two large foramina are present. One corresponds to the afferent pseudo-branchial artery, and the other to the internal carotid artery. Beyond the orbit, the postorbital section of the parasphenoid has an anterior longitudinal expansion with two ventral processes, which are projected downward and end in broad masticatory-like plates (Figure 7). The anterior of these ventral processes, also the widest and the most ventrally projected, has a heart-shaped plate that resembles those masticatory processes of basioccipital bones present in cypriniform fish (e.g., Ramaswami, 1955, figure 4); in contrast, the posterior process is arrow-shaped and points posteriorly.

The posterior longitudinal expansion of the postorbital section of the parasphenoid causes the inflection point between the orbital and postobital sections of this bone to be placed far behind the basipterygoid process, forming an angle near 120°. In general, in other ichthyodectiforms, the inflection point between the two sections of the parasphenoid occurs just behind the basipterygoid process because this bone does not have longitudinal anterior expansion in the postorbital section. *Amakusaichthys benammii* sp. nov. has an angle of about 135° formed at the base of the posterior border of the pterygoid process, between the ventral border of the orbital section of the parasphenoid and the straight line formed from the pterygoid process to the ventroposterior termination of the basicranium (as the angle of inflection of the parasphenoid in other ichthyodectiforms measures it).

Upper jaw. Each branch of the upper jaw consists of four flat and thin bones, including the premaxilla, maxilla, and two supramaxillae (Figures 5, 8). The mouth opens anterodorsally. The premaxilla is an undulating laminar rhomboidal bone widely attached to the anterior surface of the maxilla. The premaxilla has slightly convex edges and a shallow notch in the dorsal half of the medial edge. Scattered small pits ornament the labial surface of this bone. The premaxillary alveolar edge exhibits a row of 10 to 12 conical, straight, hollow, and slender small teeth. These are projected transversally from the alveolar edge, evenly sized, closely distributed, and set into deep alveoli.

The maxilla is a sinuous bone. Its alveolar section is a laminar, flat, and curved structure superficially ornamented with scattered pits and grooves ordered in an anterior-posterior radiating pattern (Figure 8). The maxillary alveolar edge is convex and shows numerous small teeth resembling the premaxillary teeth. In contrast, its toothless articular section is rectangular and robust, as long as one-fifth of the total maxillary length and at least as high as two-thirds of the maximum height of the maxilla. These two sections are inclined to

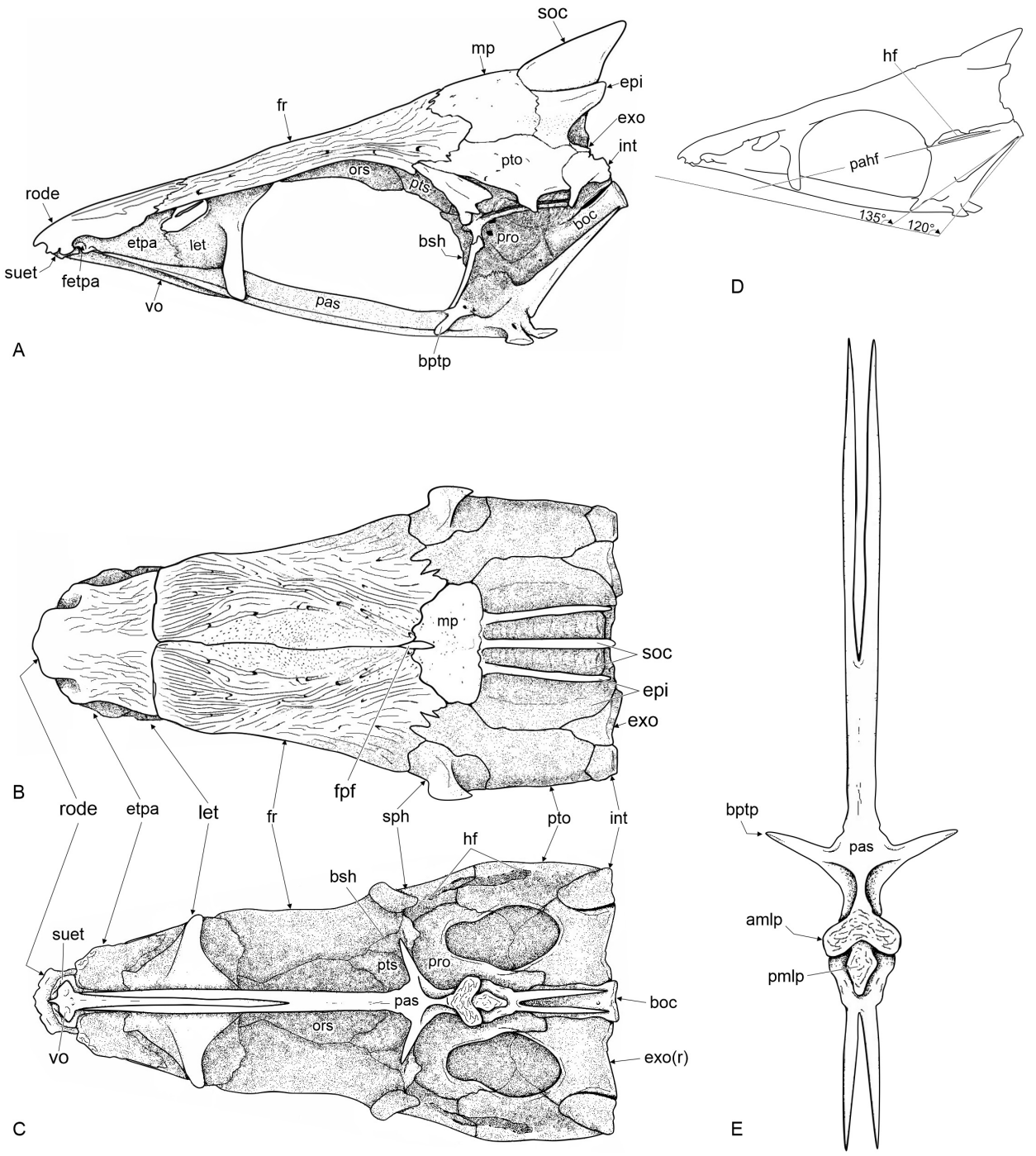

FIGURE 7. Idealized skull reconstruction of *Amakusaichthys benammii* sp. nov., from Tzimol, Chiapas, Mexico. **A,** skull in lateral view. **B,** skull in dorsal view. **C,** skull in ventral view. **D,** profile of the skull in lateral view showing the angles of parasphenoid inflection and inclination of the hyomandibular fossa. **E,** insolated parasphenoid bone in ventral view.

Abbreviations: amlp, masticatory-like processes in the parasphenoid bone; boc, basioccipital; bptp, basipterygoid process; bsh, basisphenoid; epi, epioccipital; etpa, ethmopalatine; exo, exoccipital; fetpa, articular facet of the ethmopalatine; fpf, frontoparietal fontanel; fr, frontal; hf, hyomandibular fossa; int, intercalar; let, lateroethmoid; mp, mesoparietal (=parietals fused); ors, orbitosphenoid; pahf, principal axis of the hyomandibular fossa; pas, parasphenoid; pro, proptic; pto, pterotic; pts, pteroshpenoid; rode, rostrodermethmoid; soc, supraoccipital; sph, sphenotic; suet, supraethmoid; vo, vomer.

each other, forming a dorsal inflection angle of about 235°. The maxilla shows two robust articular processes that barely protrude from the dorsal margin of its articular section. The anterior or ethmoid process of the maxilla joins the anterior ventral articular facet of the skull ethmoid region formed between the ethmopalatine and supraethmoid. On the other hand, the posterior or the maxillary palatal process articulates with the ventral part of the head of the palatine. Right at the dorsal inflection point, behind its palatal process, this bone shows a small notch, here called the maxillary palatine notch, which allocates the ventral flange of the palatine bone (below, see description of the palatine bone).

The supramaxillae are laminar and smooth bones extended above the maxilla. The anterior supramaxilla is oblong and extends along most of the alveolar maxillary section. The posterior supramaxilla is oval, with the acute anterior end overlapping most of the anterior supramaxilla.

Lower jaw. Each branch of the lower jaw consists of the dentary, angular, articular, and retroarticular (Figure 8). Together, these bones form a robust and rectangular lower jaw slightly longer than the upper jaw, about two times longer than high, and with a somewhat convex ventral edge. The high and straight mandibular symphysis is lightly inclined anterodorsally, and the coronoid process is even higher than the alveolar section of the jaw, which rises near half the jaw length. The postarticular process is small and protrudes backward.

The dentary is a deep trapezoid bone with a posterior edge forked in the lingual view and scarcely forked in the labial view (Figure 8). The ventral dentary posterior limb is extended backward up to the base of the postarticular process. The dentary shows a high symphysis, nearly half the coronoid process height. This bone shows a longitudinal thickening that protrudes near its ventral border and extends along its entire length up to the base of the postarticular process. The dentary alveolar edge is sinuous and bears a single row of numerous small teeth that resemble those already described in the upper jaw bones. Numerous pits randomly distributed are in the labial surface of the anterior third part of this bone. The mandibular sensory canal is bone-enclosed, runs longitudinally, and opens in pores near the ventral edge of the dentary.

The angular bone is a roughly triangular bone exposed in both the lingual and labial surfaces of the lower jaw (Figure 8). It has an acute anterior edge that sutures the bifid posterior dentary edge, with poor penetration in the labial view but reaching the anterior third of the mandible in the lingual view. Its labial posterior extension forms most of the postarticular process, and its lingual surface participates in the articular facet of the quadrate. The postarticular process is robust, shallow, and extends forward, representing about one-sixth of the mandibular length. The retroarticular bone is small and does not form part of the articular facet for the quadrate.

Circumorbital bones. Bones of the circumorbital series are flimsy, thin, and laminar (Figures 5–8). Unfortunately, these are poorly preserved, crushed, and broken in the referred specimens because they are usually strongly compressed against the skull. Nevertheless, these bones enclose the orbit. The antorbital is long and oblong, covering most of the skull ethmoid region. Three infraorbital bones border the orbit ventrally; the first two are rectangular, elongated, relatively small, and have ventral edges intensely fringed. The infraorbital 3 is triangular, expands over much of the cheek, and has a posterior edge intensely fringed. The infraorbital 4 is rectangular, higher than long, borders the orbit posteriorly, and has a posterior edge fringed. There is no suborbital bone behind the orbit. The dermosphenotic is a somewhat triangular and curved bone bordering the dorsoposterior part of the orbit. The single supraorbital bone is oblong and elongated and borders all the dorsal edges of the orbit.

The infraorbital sensory canal runs alongside the orbital edges of the dermosphenotic and infraorbital bones. This canal shows many branches or canaliculi that open through tiny pores at the end. A couple of large and broad sclerotic bones occupy the orbit. A thin, rounded basal sclerotic bone with serrated edges occupies the center of the orbit.

Suspensorium. Bones of the suspensorium are exposed partially in different specimens (Figures 5, 7, 8). The hyomandibular is an axe-shaped bone about 2.5 times higher than wide. Its head is a robust, long rectangular structure that nearly represents the upper third of the bone. Two large cavities arranged longitudinally pierce the hyomandibular head. The dorsal border of the hyomandibular head is somewhat sinuous but definitively forms a single articular surface for the skull. The opercular process of this bone forms shallow rounded protuberance in the basal half of the posterior margin of the hyomandibular head. The shaft of this bone is rectangular, almost vertical, slightly bent anteriorly, and as long as the anterior two-thirds of the head. This shaft has two laminar com-

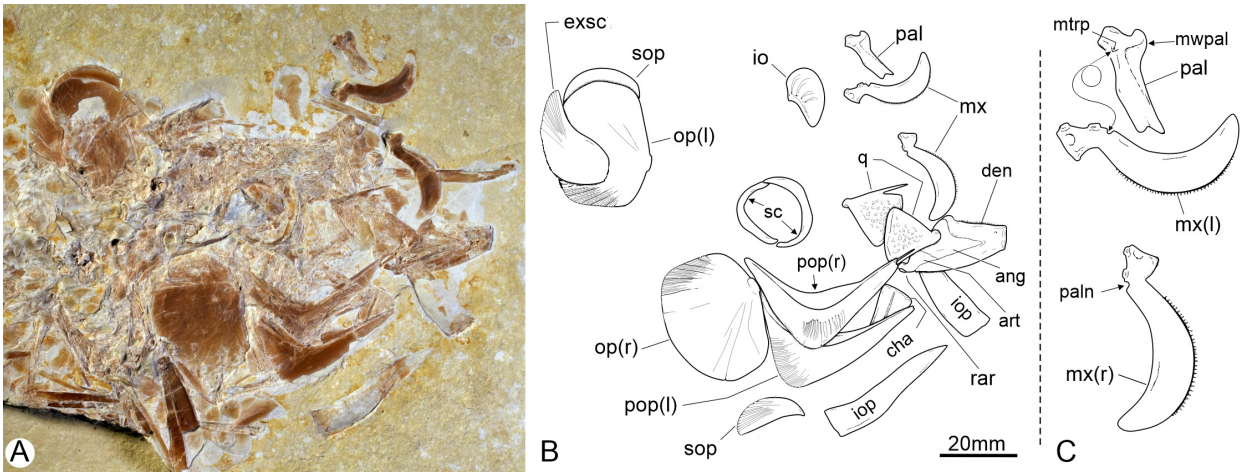

FIGURE 8. Specimen IGM 14031, *Amakusaichthys benammii* sp. nov. paratype, from Tzimol, Chiapas, Mexico. **A,** close-up of the head. **B,** idealized line drawing based on A of bones of the opercular series, pectoral fin, and jaws (the lower jaw exposes its lingual surface). **C,** idealized line drawing based on B of the palatine and maxillae.
Abbreviations: ang, angular; art, articular; cha, ceratohyal anterior; den, dentary; exsc, extrascapular; io, infraorbital; iop, interopercle; middle triangular process (of the palatine); mx, maxilla; op, opercle; pal, palatine; paln, palatine notch; pop, preopercle; q, quadrate; rar, retroarticular; sc, sclerotic bone; sop, subopercle; (l), bones of the left side; (r), bones of the right side.

ponents; the lateral one forms a narrow and thick external surface with superficial apicobasal shallow grooves and a posterior deep preopercular groove; in contrast, the medial component forms a smooth internal wing, thinner, mostly extended anteriorly, with a dorsal large foramen for the hyomandibular nerve.

The quadrate bone is flat, triangular, and strongly inclined posteriorly, with its anterior and posterior edges almost vertical and horizontal, respectively (Figures 7–8). The quadrate articular head is short and does not overhang from the anterior edge of the bone; this joints the lower jaw a little forward of the orbit and below the lateroethmoid bone; and its articular surface is oval, vertically exposed, broad, and consists of two malleoli separated by a wide groove arranged on a lateral-dorsal to the medial-ventral axis. Just behind the articular head, the ventral border of this bone has a slight broadening with a shallow notch, in which the dorsal posterior termination of the post-articular process of the lower jaw rests. The quadrate has a slightly curved edge meeting the metapterygoid bone. The posterior process of the quadrate is nail-shaped and as high as the quadrate body. The symplectic is wedge-shaped, lateromedially flat, nearly 2.5 times longer than high, and only slightly shorter than the quadrate.

The ectopterygoid is triangular, gracile, and toothless (Figure 5). This bone has a ventral horizontal limb attached to the anterior edge of the quadrate and a vertical anterior dorsal limb attached to the ventral edge of the endopterygoid and the terminal end of the palatine. The endopterygoid is a rectangular bone extending above the dorsal anterior half of the quadrate dorsal edge and below the orbital anterior half and the lateroethmoid, and its anterior termination dorsally borders the dorsoposterior half of the palatine. The lingual surface of the endopterygoid is spongy endochondral bone and bears petite small tubercular teeth.

The metapterygoid is an elongated trapezoidal bone, higher anteriorly and with curved edges (Figure 9). Its dorsal edge is slightly concave and extends below the posterior half of the orbit. Its ventral edge is concave and extends between the symplectic and the hyomandibular shaft. Its posterior edge is shallow, almost straight, and reaches the medial internal wing of the hyomandibular just behind the ventroposterior part of the orbit. Finally, its anterior edge is high, slightly concave, anterodorsally tilted, and attaches to the posterior edge of the quadrate.

The palatine is a long rectangular bone, slightly dorsoposteriorly tilted, placed below the skull ethmoid region and nearly as long as the lateroethmoid (Figures 5, 7, 8). Anteriorly, the articular end of the palatine forms a robust, rectangular head. Its articular head is sinuous anteriorly, and its articular facet for the ethmopalatine is somewhat protruding and rounded. In contrast, its articular facet for the posterior articular process of the max-

illa is practically flat. Behind the articular head, this bone shows a semicircular medial wing protruding dorsally and a thick middle triangular process to attach the palatine notch of the maxilla.

Opercular bones. The opercular series of this fish is complete and includes four laminar bones (Figures 7–8). The opercle is an oval fan-shaped bone, about 1.6 times higher than long, with a rounded and thin contour except for its straight and thickened anterior border, which only represents about half the height of the bone. The posterior and dorsal borders of the opercular are fringed, especially in the dorsoposterior part. The articular facet for the hyomandibular is at the dorsal end of the anterior border of the bone. This facet is almost flat, exposed on the anterior opercular edge, and protruding anteriorly. The ornament of this bone consists of scattered pits and short grooves ordered in radiating pattern from the articular facet for the hyomandibular.

The preopercle is an inverted-L-shaped bone with dissimilar limbs, forming an inner angle slightly higher than 90° and a posteroventral corner somewhat prominent (Figures 7–8). The height of the preopercle barely reaches the opercular articular facet for the hyomandibular. Here, the vertical preopercular limb is relatively short, slightly broad, and has a posterior edge intensely fringed. On the contrary, the horizontal preopercular limb is two times longer than the height of the vertical preopercular limb, slender, and its edges are entirely harmonious (= not fringed). The smooth preopercular median shelf shows a sinuous dorsal edge. The preopercular sensory canal runs near the inner edge of this bone and is intensely branched, forming a peculiar superficial pattern on the horizontal limb of deep grooves that are numerous and parallel.

The subopercle is a semi-oval bone as long as the opercle, with a rounded contour and a slightly concave dorsal border (Figures 7–8). The subopercular anterior ascending process is triangular and shallow. Numerous parallel and shallow radiating grooves ornament the subopercle bone laterally, from its anterior region to its ventroposterior fringed edge. Below the horizontal preopercular limb, the interopercle is an elongated and somewhat sinuous triangular bone that is acute anteriorly, nearly four times longer than high, and has a straight posterior edge.

Branchiostegal rays and branchial arch. Elements of the branchial arch are partially covered. Both hypohyal bones are rectangular, thick, lateromedially flat, smooth, and subequal-sized. The dorsal hypohyal is slightly higher than the long, and the ventral hypohyal is about 1.5 times higher.

The ceratohyal bones are flat (Figure 8). The anterior ceratohyal is rectangular, long, nearly two times longer than high, and has no beryciform foramen. The posterior ceratohyal is triangular, tapered posteriorly, broad anteriorly, and has a straight edge to join the anterior ceratohyal. Ceratohyal bones have a medial longitudinal groove for the afferent hyoidean artery. The interhyal is a short dorsal rod-like bone joining the posterior tip of the posterior ceratohyal. The urohyal is a complex elongated bone with an anterior small head, a lateral basal flat wing, and a rectangular medial dorsal flange.

A series of at least 15 elongated and dorsally bent branchiostegal rays are articulated proximally to the lateral surfaces of the ceratohyal bones; the most anterior ones are short bones and thin as threads; the subsequent branchiostegal rays become more prolonged, broader, and the last three spathiform.

Branchial bones are covered by more superficial or strongly disarticulated and dispersed in the available specimens. Therefore, the structure of the gill arch is unknown. Despite this, at least some of the pharyngobranchial bones have minute teeth.

Axial skeleton. The vertebral column consists of 78 total centra, including 54 abdominals, 22 preurals, and two urals (Figures 1, 10; Table 1). The centra are cylindrical, well ossified, and have deep concave intervertebral surfaces perforated by a tiny central notochordal foramen. Along the abdominal and the anterior half caudal region, the centra are slightly longer than high in lateral view. Subsequent caudal centra become progressively smaller and shorter; the preural centra 1–5 are slightly higher than long. A couple of elongated oval perforations carve the lateral surfaces of all these centra except for the first abdominal and at least the preural 1, which are superficially smooth.

The ribs are long, curved, and evenly widened bones enclosing most of the abdominal cavity (Figure 10). The ribs are somewhat laterally flat bones laterally carved by a shallow apicobasal groove and have robust articular heads. The first abdominal centrum lacks ribs; the abdominal centra 2–42 have a pair of associated ribs directly in the lateroventral facets of the centra; the ribs and abdominal centra 43–54 joint with sharp autogenous parapophyses that attach with the lateroventral facets of the respective centra. These parapophyses are ventrally projected and increase in size in the anteroposterior order; the height of the posterior

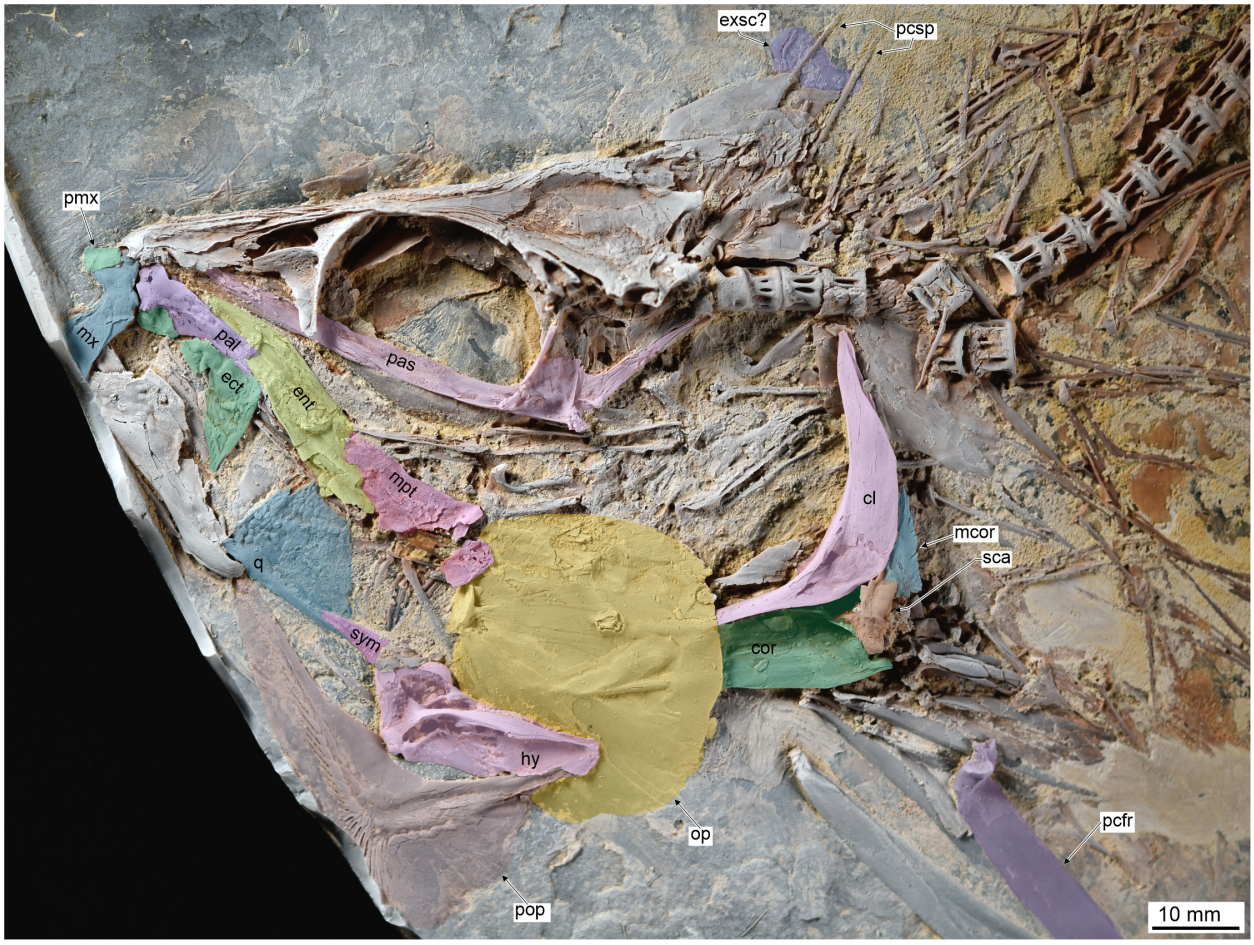

FIGURE 9. Head and anterior part of the trunk of IGM 14027b, the counterpart of the holotype of *Amakusaichthys benammii* sp. nov. from the Tzimol Quarry Chiapas, Mexico, transferred to resin and coated with magnesium. **Abbreviations:** cl, cleithrum; cor, coracoid; ect, ectopterygoid; ent, entopterygoid; exsc, extrascapular; hy, hyomandibula; mcor, metacoracoid; mpt, metapterygoid; mx, maxilla; op, opercle; pal, palatine; pas, parasphenoid; pcfr, pectoral fin ray; pcsp, postcranial spines; pmx, premaxilla; pop, preopercle; q, quadrate; sca, scapula; sym, symplectic.

parapophyses equals the length of one and a half abdominal centra. The posterior eight or nine pairs of ribs become more petite and articulate with small parapophyses of the respective centra.

All the neural and hemal arches are autogenous and tightly attached to the centra (Figures 2, 10). These arches are shallow, almost as long as the respective centrum, and have noticeably large processes to attach the centra. Along the vertebral column, the elongated articular processes of each neural and hemal arches joint the deep cavities or facets on the dorsal and ventral surfaces of the respective centrum. The spines are long, sharp, inclined, and curved posteriorly; among these, the most anterior 35–40 are deeply bifid. In the anterior two parts of the caudal region (up to the vertebrae 60–62), the neural spines are slightly curved and tilted posteriorly, forming an arc two times higher than the respective centrum and as long as the next two posterior centra. Beyond that, the neural spines become shorter, straighter, and more inclined. Preural neural arches 2–7 have thick neural spines and dorsoanterior saddle-shaped processes that extend anterodorsally, reaching and supporting the neural spine of the adjacent anterior preural centrum. These saddle processes become smaller in these centra, following the posterior-anterior order, whereas the respective neural spines become gradually more vertical. At least the neural spines of preural arches 2 and 3 present a complex articulation with their corresponding saddle-shaped processes; these spines have a callosal process allocated within a middle cavity in the dorsoanterior surface of the respective saddle process. This cavity has not yet been directly observed; however, the saddle process becomes broad and protrudes laterally around its contact with the callosal process region. Although less

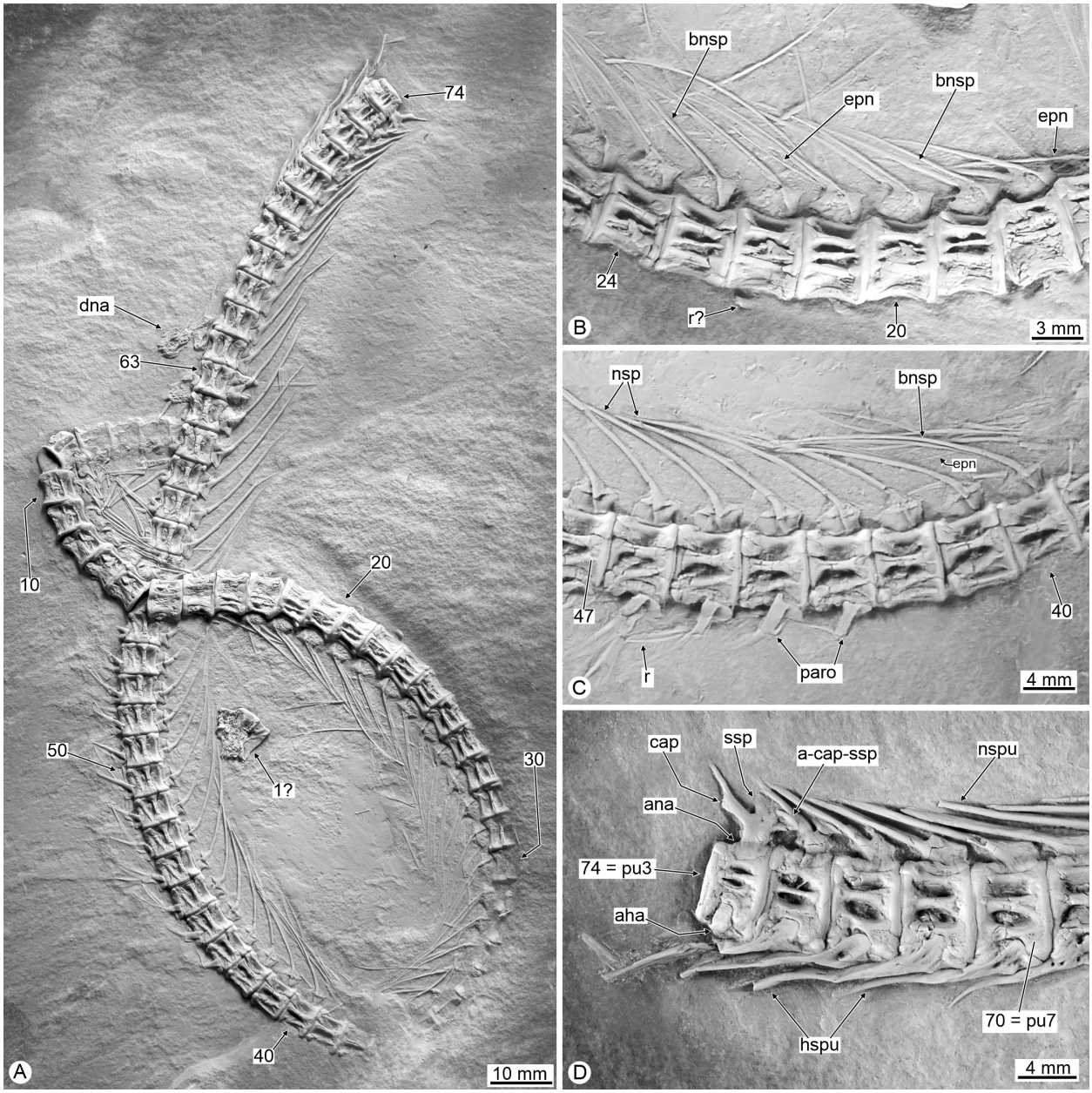

FIGURE 10. IGM 14034, paratype of *Amakusaichthys benammii* sp. nov., transferred to resin and coated with magnesium, showing a nearly articulated vertebral column and some associated bones. **A,** complete specimen. **B,** anterior abdominal centra with bifid neural spines. **C,** abdominal region in which the neural spines bifid change to normal or non-bifid neural spines. **D,** posterior caudal centra.

Abbreviations: numbers show the position of the centra in anterior to posterior order; a-cap-ssp, articulation between the callosal process of the neural spine and the dorsoanterior cavity of the saddle-shaped process; aha, autogenous hemal arch; ana, autogenous neural arch; bnsp, bifid neural spines; cap, callosal process; dna, disarticulated neural arch; epn, epineural; hspu, hemal spine of preural centrum; nsp, neural spine (non-bifid); nspu, neural spine of preural centrum; paro, parapophysis; pu, preural centrum; r, rib; ssp, saddle-shaped process; ssp, saddle-shaped processes of preural centrum.

inclined backward, the hemal spines are almost symmetrical images opposite the hemal spines. The hemal spines of preural 2–5 are noticeably thicker than the preceding ones.

An indeterminate number of flat, long, and straight-ended supraneural bones are along the predorsal region. These bones appear to be placed in relation 1 to 1 with the neural spines without pen-

etrating the interneural spaces. The epineurals are elongated thread-like bones that rise from the lateral surface of the neural arches, are as long as 8–12 centra in the anterior abdominal centra, and become progressively shorter in subsequent abdominal centra. There are no epipleural nor epicentral ossified.

Pectoral girdle and fins. On each side of the body, this fish has a large and flat triangular medial supratemporal or extrascapular bone (sensu Patterson and Rosen, 1977, p. 93) that lies over the occiput and the dorsal part of the pectoral girdle. This bone expands posteriorly, has a deeply fringed rear, and carries the supratemporal canal alongside its anteroventral edge (Figures 5–9).

The posttemporal is a roughly Y-shaped bone with broad limbs (Figure 5). The supracleithrum is rectangular, tilted, and slightly curved dorsoanteriorly. In these bones, the posttemporal sensory canal opens in large pores near the tip of the posttemporal limbs and in and alongside the dorsal half of the supracleithrum. Two large scale-like postcleithra are present behind the dorsal limb of the cleithrum.

The cleithrum is a crescent-shaped bone in lateral view (Figure 9). Its horizontal and vertical limbs are similarly slender, elongated, and acute-ended. The horizontal limb has a poorly expanded lateroventral surface and barely convex ventral edge; on the contrary, the vertical limb has a larger lateroposterior surface and a sinuous posterior edge with a dorsal concavity to allocate the postcleithra. The intersection of these limbs forms an anterior barely obtuse angle nearly to 95–100°. The coracoid is an elongated triangular bone, broad posteriorly, almost four times higher than long, and its anterior end is ahead of the horizontal cleithrum limb. Probably, the ventral parts of both coracoids meet in the midline. The scapula is a small bone located in the ventroposterior corner of the cleithrum. The mesocoracoid is a triangular thick bone covered by the posterior part of the cleithrum just above the pectoral fin base.

The large trapezoidal pectoral fin rises near the ventral edge of the trunk and extends in the anterior fifth of the abdomen (Figure 9). The fin consists of about 12 rays with robust heads joining the distal ends of at least five short, robust pectoral radials that join the scapula. The most anterior pectoral rays are saber-shaped bones with a broad laminar body distally branched and segmented. Peculiarly, the sutures between the segments are intensely zigzagging or step-like and strongly tilted backward. The first ray is the largest, and its base is about two times wider than the second ray; subsequent rays become shorter and have less width.

Pelvic girdle and fins. This fin is probably tiny, triangular, and rises in the posterior half of the trunk, at 70% of SL, below the abdominal centrum 50 (Figures 2, 11, 12; Table 1). The fin has eight broad rays extending below four to five abdominal centra (abdominal centra 51–55). Among these rays, the first one is the widest, is segmented, and branched distally as the first pectoral fin ray. The proximal ends of all pelvic rays articulate directly with the posterior border of the pelvic bone, except for the first two rays that articulate two intermediate robust and short radials.

The pelvic girdle consists of two elongated pelvic bones, laying beneath three abdominal centra (abdominal centra 47–50) and united only by their stout rectangular median processes (Figure 11). In the dorsoventral view, each pelvic bone is a complex axe-shaped structure that is expanded posteriorly and has an anterior handle that is thin, short, and sharp-ended. The central part of the pelvic bone consists of a longitudinal rod-like structure that is straight and thick. A rectangular lateral wing extends laterally from the rear to two-thirds of the central part; however, this bone has no medial wing developed in the counterpart. The ventral external wing is a thickened and shallow trapezoidal structure projected ventrally from the posterior third of the central part of the pelvic bone.

The posterior end of the pelvic bone is remarkably thick (Figure 11). A rectangular medial process occupies the fifth posterior part of the medial border. The bone has no posterior process. In opposition, the posterolateral corner of the lateral wing presents a lateral process forming two anteroposteriorly compressed triangular prominences protruding ventral and dorsally. The posterior border of the pelvic bone is sinuous and has a conspicuous posterior projection at its medial end.

Dorsal fin. This fin is triangular, short, and located far in the back of the trunk and slightly behind the origin of the anal fin, opposing the acuminate lobe of the anal fin (Figures 2, 4, 11). Although none of the specimens studied show a complete dorsal fin, the specimen IGM 14028 has 13 rays forming part of this fin, including a short unbranched ray plus 12 branched and segmented rays. The dorsal pterygiophores series that supports this fin includes 13 proximal pterygiophores and uncertain numbers of distal and medial pterygiophores. The anterior proximal pterygiophores are so long that they penetrate the spaces between the neural spines located below; behind, the posterior proximal ptery-

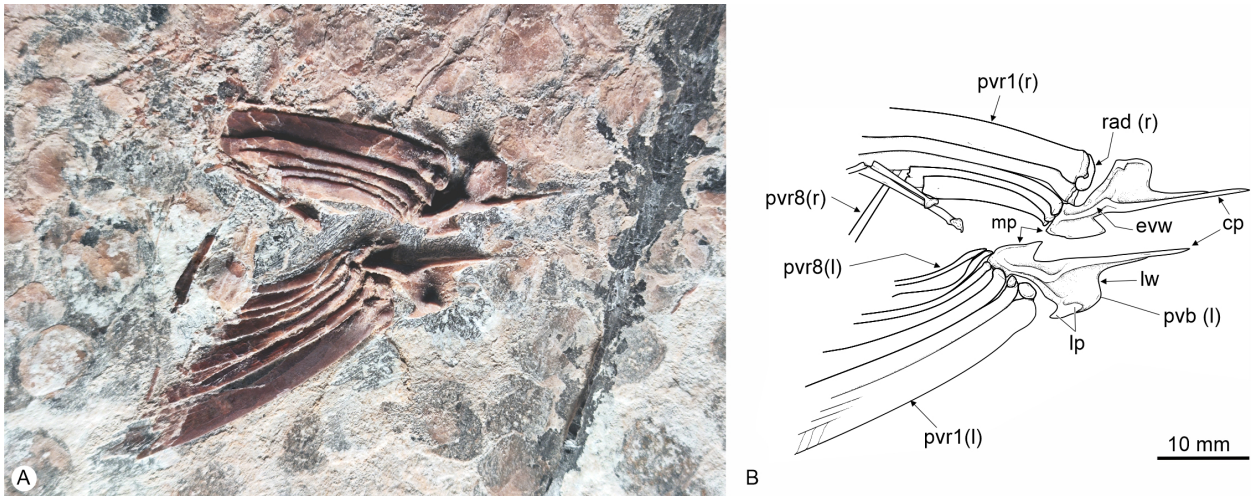

FIGURE 11. Pelvic girdle (in ventral view) of *Amakusaichthys benammii* sp. nov. from the Campanian marine deposits of the Angostura Formation exploited in the Tzimol Quarry, Comitán Municipality, Chiapas, southeastern Mexico. **A,** IGM 14027a under white light. **B,** idealized line drawing of A.
Abbreviations: cp, central part of the pelvic bone; evw, external ventral wing; lp, lateral process; lw, lateral wing; mp, medial process; pvr, pelvic fin ray; rad, radian; (l), elements of the left side; (r), elements of the right side.

giophores become progressively shorter. The first dorsal proximal pterygiophore is forked at the base and has a long anterior projected anteroventrally.

Anal fin. This fin is long, acuminated, and located far in the back of the trunk and slightly ahead of the dorsal fin (Figures 2, 4, 12). The specimen IGM 14028 has 19 rays forming part of this fin, including a short unbranched ray plus 18 branched and segmented rays. The anal pterygiophores series that support this fin includes 18 proximal pterygiophores and uncertain numbers of distal and medial pterygiophores. All the proximal pterygiophores are long rod-like structures that are shorter in the anterior to posterior order; among these, the anterior two or three anal proximal pterygiophores are so long that they penetrate the interhemal spaces located above.

Caudal fin and skeleton. The caudal fin is deeply forked and consists of two triangular lobes opposed, similarly shaped, and markedly dissimilar in size (Figures 2, 4). Considering the length of the principal axes of both lobes, the ventral lobe is nearly 1.5 times longer than the dorsal one.

The caudal formula is x+I+8—9+I+viii. Here, the procurrent rays are long and unsegmented, both principal rays are notably broad, and the inner rays are intensely branched (Figures 2, 12). The principal and most inner rays in both lobes show an intense segmentation, in which the segments are uniformly rhomboid, narrow, and so distally tilted that each segment overlaps nearly 70–80% of the successive segment. The sutures between these

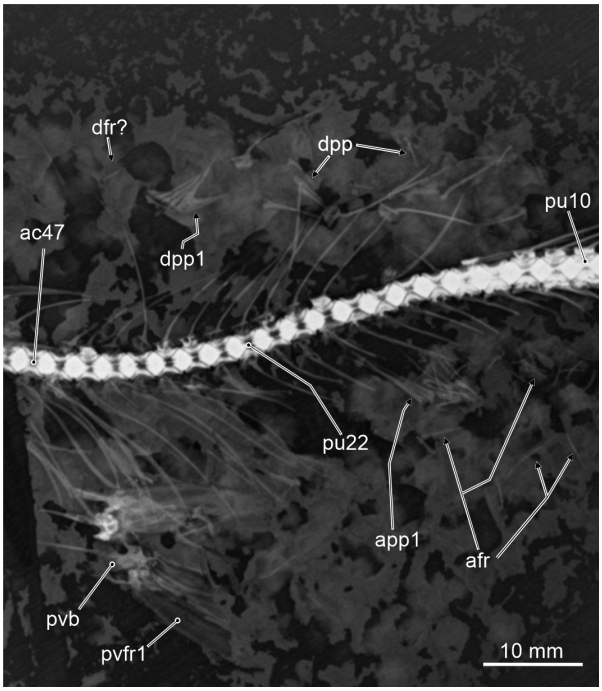

FIGURE 12. X-ray image of the unpaired fins preserved in IGM 14027b, holotype of *Amakusaichthys benammii* sp. nov. from the Campanian marine deposits of the Tzimol Quarry, Comitán, Chiapas, southeastern Mexico.
Abbreviations: ac, abdominal centrum; afr, anal fin ray; app, anal proximal pterygiophore; dfr, dorsal fin ray; dpp, dorsal proximal pterygiophore; pu, preural centrum; pvb, pelvic bone; pvfr, pelvic fin ray.

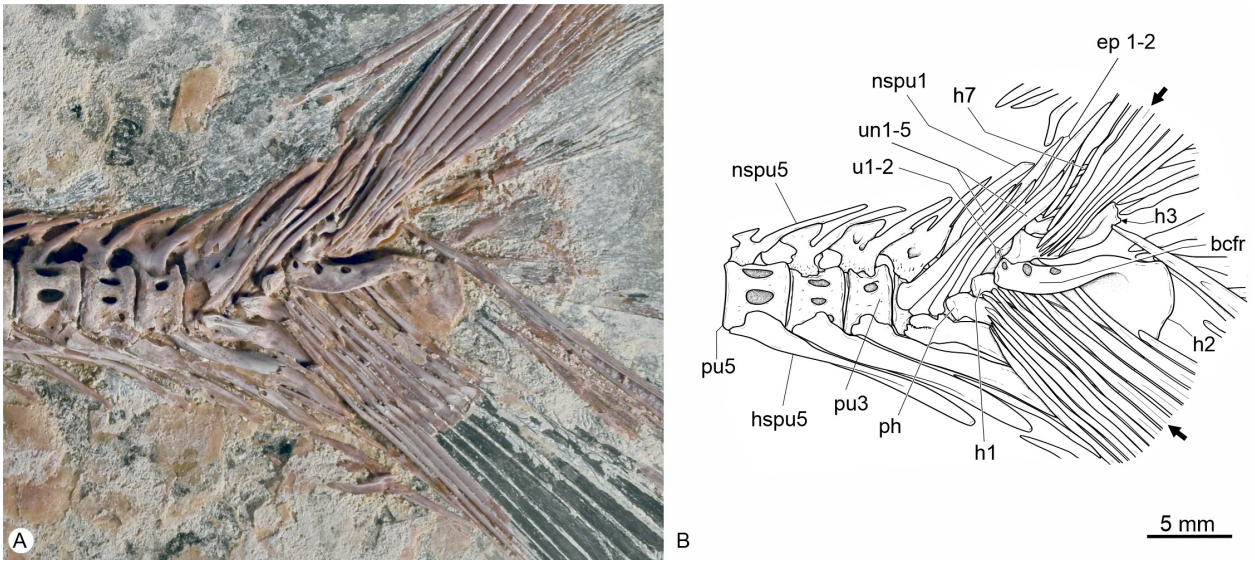

FIGURE 13. Caudal fin IGM 14027, holotype of *Amakusaichthys benammii* sp. nov. from the Campanian marine deposits of the Angostura Formation exploited in the Tzimol Quarry, Comitán Municipality, Chiapas, southeastern Mexico. **A,** part of the specimen (IGM 14027b) transferred to resin and observed under white light. **B,** idealized line drawing of A.

Abbreviations: bcfr, blanket-corner folded ridge of hypural 2; ep, epural; h, hypural; hspu, neural spine of preural centhrum; nspu, neural spine of preural centhrum; ph, parhypural; pu, preural centhrum; u, ural centhrum; un, uroneural; black arrows show principal fin ray in both dorsal and ventral caudal fin lobes.

segments are parallel and straight when viewed with the naked eye, but when a microscope is used, such sutures are shallow and intensely zigzagging. In addition, the rays that form the long part of both lobes extend anteriorly and cover much of the caudal skeleton bones, so the distal ends of the hypurals are unknown.

The caudal skeleton involves the spines of the preural centra 1–4, the parhypural, two ural centra, five uroneurals, seven hypurals, and probably only two epurals (Figures 12–13). Neural spines of preurals 1 and 2 and the ural 1 support the anterior ends of the caudal dorsal rays; these spines are progressively enlarged and thick, somewhat curved, and tilted nearly 45°, contrasting with those of previous preurals that are shorter, thinner, and tilted more horizontally. The hemal spines of preural centra 1–4 (including the parhypural) support the anterior end of ventral caudal rays. These somewhat sinuous hemal spines are thicker, longer, and more horizontally inclined than previous preurals. Among these, the hemal spine of preural centra 2 and the parhypural lie nearly horizontal below the caudal fin rays and have noticeably robust articular heads that protrude laterally.

There are five flat uroneurals, almost straight, parallel, and inclined, about 45° covering the lateral surface of the urals and preurals 1 and 2 (Figure 13). The first uroneural is the most robust; its anterior end is round, expanded, and sloping anteriorly, while its dorsal part becomes slender, covers much of the neural spine of ural 1, and is shorter than the neural spine of preural 1. The posterior four uroneurals are thinner, equally long, and progressively located a little more dorsally. Between uroneurals 2 and 3, there are two robust and needle-like epurals dorsally extended beyond the distal end of the neural spine of ural 1. There are no urodermals. Both urals and preural 1 are almost entirely covered.

The anterior ends of the caudal fin rays cover most of the seven hypurals (Figure 13). Hypurals 1–4 have robust heads protruding laterally, as the parhypural; however, the heads of these hypural are so broad that they are in contact with each other and enclose part of the corresponding ural. It is impossible to determine whether the head of hypural 1 also has a ball-and-socket joint with ural 1, as in other ichthyodectiforms. The hypurals 1 and 2 attach the ural 1 and project posteroventrally, whereas the hypurals 3–7 joint the ural 2 and project posterodorsally, so there is a narrow and deep caudal diastema between the hypurals 2 and 3. The main axes of the bones of both hypural groups are poorly tilted posteriorly below and above the longitudinal axis of the vertebral column.

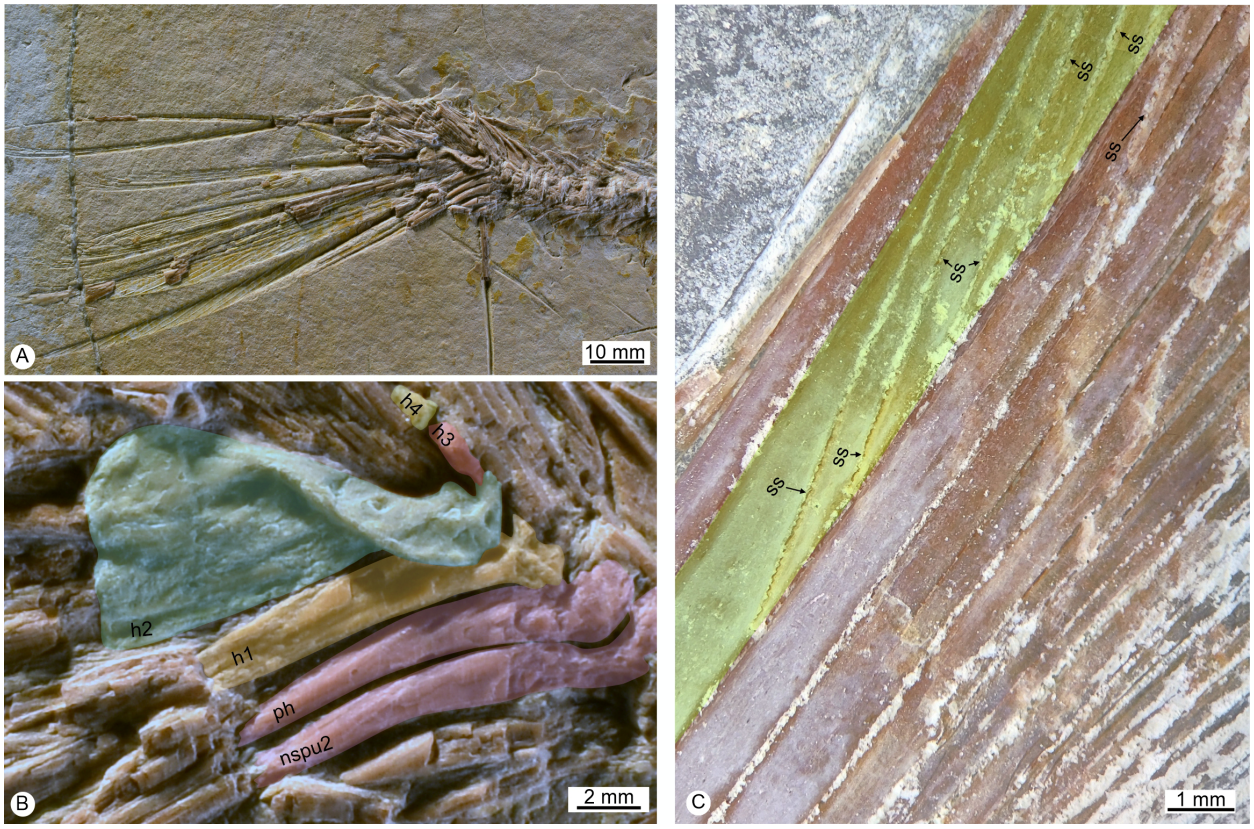

FIGURE 14. Caudal fin of *Amakusaichthys benammii* sp. nov. from the Campanian marine deposits of the Angostura Formation exploited in the Tzimol Quarry, Comitán Municipality, Chiapas, southeastern Mexico. **A,** general view of IGM 14035, paratype of the specimen under white light with the anterior tips of the ventral caudal rays removed. **B,** close-up of A with some bones of the caudal skeleton are colored. **C,** close-up of the principal ray (in green) in the dorsal lobe of the caudal fin of IGM 14027b, under white light, showing the suture between its segments.
Abbreviations: h, hypural; nspu, neural spine of preural centhrum; ph, parhypural; ss, suture between the ray segments.

All the hypurals are elongated trapezoidal bones slightly expanded posteriorly, except for hypural 2, a large triangular or fan-like structure with a noticeably expanded rear and the dorsal and posterior edges sinuous (Figures 12, 14). The dorsal edge of hypural 2 lies horizontally, and its articular broad rounded head protrudes laterally and contacts the articular heads of hypurals 1 and 3. Additionally, the hypural 2 has a peculiar ridge extended in the anterior four-fifths of its dorsal edge. It extends laterally and folds ventrally, forming a triangular structure resembling the folded corner of a blanket on the bed. This blanket-corner-folded ridge has a sinuous ventral edge, is pierced laterally by three oval holes, and roofs an elongated cavity that houses the proximal ends of the ventral caudal rays.

The length of hypural 3 is nearly three-quarters of hypural 2 (Figure 13). The articular head of this hypural is also robust but quadrangular shaped and as broad as that of hypural 2. Its ventral edge is sinuous and shows a blanket-corner-folded ridge like that of hypural 2 but less developed and extended along the entire bone. The articular head of hypural 4 is broad but smaller than the head of hypural 3. The edges of hypurals 5–7 are between and below the dorsal caudal rays.

Scales. Thin cycloid scales strongly imbricated cover the entire trunk, the posterior part of the head, and the base of the caudal fin rays. The scales are circular near the ventral and dorsal edges of the trunk, but toward the flanks, these become oval, about 1.5 times higher than long. The ornaments of the scales include numerous concentric circulii, punctae in the anterior half, and straight and parallel anterior radii, long on the anterior edge and short on the posterior one (Figure 15).

Most scales are disarticulated and scattered around the skeleton in the fossils studied here.

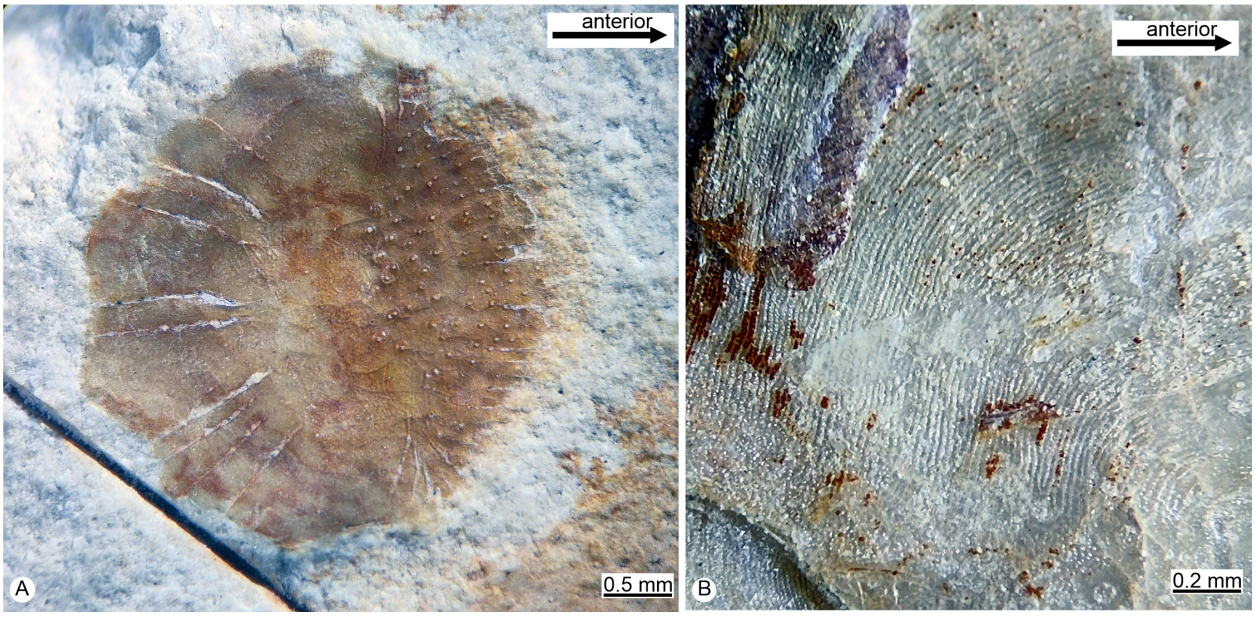

FIGURE 15. Scales of *Amakusaichthys benammii* sp. nov. from the Campanian marine deposits of the Angostura Formation exploited in the Tzimol Quarry, Comitán Municipality, Chiapas, southeastern Mexico. **A,** internal surface of an isolated scale from the dorsal trunk edge of IGM 14033a. **B,** external surface of imbricated scales in the lateral part of the trunk of IGM 14036.

This preservation avoids the recognition of the scale lines that cover the body. Some scales longitudinally perforated by the lateral line canal are present near the vertebrae, revealing that this sensory canal may extend along the trunk near the vertebral column.

DISCUSSION

Phylogenetic Considerations

Recent paleontological studies have significantly expanded the knowledge of the taxonomic diversity of Ichthyodectiformes. Without excluding some questionable species, today, the order involves 75 species representing 44 genera (Table 2); however, many of their interrelationships are still unclear. In the present scenario, undertaking a comparative osteological exercise to perform a comprehensive phylogenetic analysis of this group is challenging because it requires an accurate anatomical review of different problematic species represented by scarce fossils or poorly studied. Although an effort of such magnitude is beyond the scope of the present work, here, the relationships of *Amakusaichthys benammii* sp. nov. are explored phylogenetically based on a morphological data set gathered and updated by previous authors (see the section Material and Methods of this work).

In this section of the manuscript, the observations documented show that the species of three genera — *Bardackichthys* Hacker and Shimada, 2021; *Jinjuichthys* Kim, Chang, Wu, and Kim, 2014; and *Mesoclupea* Ping and Yen, 1933 — are not ichthyodectiforms. This work does not include data generated on the direct review of specimens of these three genera. Therefore, the phylogenetic relationships of *A. benammii* are evaluated here through two phylogenetic analyses; one includes these genera, and the other excludes them. The results of these analyses are presented below.

Recently, Hacker and Shimada (2021) named the family Bardackichthyidae within the suborder Ichthyodectoidei to include *Bardackichthys, Heckelichthys,* and *Amakusaichthys goshouraensis*. A detailed review of the anatomical features and figures included in their description of *Bardackichthys* shows the following inconsistencies. Although its authors claim that *Bardackichthys* presents the diagnostic features of the order Ichthyodectiformes (the uroneurals cover the lateral surface of the last preural and ural centra, the presence of an ethmopalatine bone in the floor of the nasal capsule, and the most anterior rays in the pectoral and pelvic fins are saber-like shaped); their illustrations show different features challenging the convenience of considering *Bradackichthys* as a member of the order Ichthyodectiformes, and consequently, the naturalness of the family Bardackichthydae. In *Bradackichthys*, the uroneurals cover only the dorsal

TABLE 2. Nominal valid species described or referred to the order Ichthyodectiformes.

Species	Age. Distribution.
Africathrissops weileri Taverne, 2010	Aptian. Gabon
Aidachar pankowskii (Forey and Cavin, 2007)	Cenomanian. Morocco
Aidachar paludalis Nessov, 1981 (see Mkhitaryan and Averianov, 2011)	Turonian. Uzbekistan
Allothrissops mesogaster (Agassiz, 1833)	Early Tithonian. Germany
Allothrissops regleyi (Thiollière, 1854)	Kimmeridgian. Francia
Allothrissops salmoneus (Blainville, 1818)	Kimmeridgian. Europe
Altamuraichthys meleleoi Taverne, 2016	Campanian-Maastrichtian. Italy
Amakusaichthys benammii Alvarado-Ortega, this work	Campanian, Mexico
Amakusaichthys goshouraensis Yabumoto, Hirose, and Brito, 2018	Santonian. Japan
Antartithrissops australis Arratia, Scasso, and Kiessling, 2004	Tithonian. Antarctica
Ascalabothrissops voelkli Arratia, 2000	Kimmeridgian. Germany
Bardackichthys carteri Hacker and Shimada, 2021	Cenomanian. USA
Capassoichthys alfonsoi Taverne, 2015	Campanian-Maastrichtian. Italy
Chirocentrites coroninii Heckel, 1849	Cenomanian. Slovenia
Chirocentrites neocomiensis (Pictet, 1858)	Hauterivian. France
Chirocentrites? *calvolini* Costa, 1865	Albian. Italy
Chiromystus alagoensis Jordan, 1910	Early Cretaceous, Brazil
Chiromystus guinensis (Weiler, 1922)	Aptian. Africa
Chiromystus mawsoni Cope, 1885	HauterivianAlbian. Brazil
Chuhsiungichthys japonicus Yabumoto, 1994	Hauterivian-Barremian. Japan
Chuhsiungichthys tsanglingensis Lew, 1974	Early Cretaceous. China
Chuhsiungichthys yanagidai Yabumoto, 1994	Hauterivian-Barremian. Japan
Cladocyclus gardneri, Agassiz, 1841	Aptian. South America
Cladocyclus geddesi Berrell, Alvarado-Ortega, Yabumoto, and Salisbury, 2014	Albian. Australia
Cladocynodon araripensis Mayrinck, Ribeiro, Assine, and Spigolon, 2023	Aptian. Brazil
Cooyoo australis (Woodward, 1894)	Albian. Australia
Dugaldia emmilta Cavin and Berrell, 2019	Albian. Australia
Eubiodectes libanicus (Pictet and Humbert, 1866)	Cenomanian. Lebanon
Faugichthys loryi Taverne and Chanet, 2000	Albian. France
Furloichthys bonarellii Taverne and Capasso, 2018	Cenomanian. Italy
Garganoichthys alfonsoi Taverne, 2009	Santonian. Italy
Gillicus arcuatus Cope, 1875	Albian-Campanian. North America
Gillicus serridens Woodward, 1901	Albian. England
Ghrisichthys bardacki (Cavin, 1997)	Turonian. Morocco
Gwawinapterus beardi Arbour, Currie, 2011	Late Cretaceous. Canada
Heckelichthys preopercularis Baños-Rodríguez, González-Rodríguez, Wilson, and González-Martínez, 2020	Albian-Cenomanian limit. Mexico
Heckelichthys microdon (Heckel, 1849)	Barremian-Cenomanian. Europe
Heckelichthys vexillifer (Heckel, 1856)	Neocomian. Morroco
Ichthyodectes ctenodon (Leidy, 1857)	Albian-Campanian. USA
Ichthyodectes minor Dixon, 1850	Albian-Campanian. Europe
Itaparica woodwardi (Silva-Santos, 1949)	Hauterivian-Albian. Brazil
Jinjuichthys cheongi Kim, Chang, Wu, and Kim, 2014	Albian. Japan
Mesoclupea showchangensis Ping and Yen, 1933	Early Cretaceous. China

TABLE 2 (continued).

Species	Age. Distribution.
Occithrissops willsoni Schaeffer and Patterson, 1984	Bathonian. USA
Ogunichthys triangularis Alvarado-Ortega and Brito 2010	Aptian?. Brazil
Pachythrissops laevis Woodward, 1919	Purbeckian. England
Pachythrissops propterus (Wagner, 1863)	Tithonian. Germany
Postredectes harranaensis Kaddumi, 2009	Maastrichtian-Paleocene?, Jordan
Proportheus kameruni Jaekel, 1909	Turonian-Cenomanian. Africa
Prosaurodon pygmeus (Loomis, 1900) (see Stewart, 1999)	Santonian-Campanian. USA
Prymnetes longiventer Cope, 1871	Early Cretaceous?. Mexico
Saurocephalus lanciformis Harlan, 1824	Turonian-Maastrichtian. America
Saurocephalus woodwardi Davies, 1878	Upper Cretaceous. Europe
Saurodon elongatus Taverne and Bronzi 1999	Campanian-Maastrichtian. Italy
Saurodon intermedius Newton, 1878	Cenomanian. England
Saurodon leanus Hays, 1830	Cenomanian-Campanian. North America
Sultanuvaisia antiqua Nessov 1981	Late Cretaceous. Kazakhstan
Thrissops cephalus Agassiz, 1844	Oxfordian. England
Thrissops cirinensis Nybelin, 1964 (see Taverne, 1977)	Kimmeridgian. Germany
Thrissops costalis Egerton, 1845	Oxfordian. England
Thrissops curtus Woodward, 1919	Portlandian. England
Thrissops exiguus Bassani, 1879	Cenomanian. Slovenia
Thrissops formosus Agassiz, 1833 (see Taverne, 1977)	Kimmeridgian. Germany
Thrissops gracilis Heckel, 1849	Cenomanian. Slovenia
Thrissops portlandicus Woodward, 1895	Portlandian. England
Thrissops rochei Sauvage, 1893	Kimmeridgian. France
Thrissops subovatus Münster (in Agassiz, 1844) (see Taverne, 1977)	Kimmeridgian. Germany
Thrissops volganensis Koslov, 1928	Portlandian. Russia
Unamichthys espinosai Alvarado-Ortega, 2004	Albian. Mexico
Vallecillichthys multivertebratum Blanco and Cavin, 2003	Turonian. Mexico
Verraesichthys bloti Taverne, 2010	Aptian. Africa
Xiphactinus audax Leidy, 1870	Cenomanian-Campanian. North America
Xiphactinus gaultinus Newton, 1877	Albian-Cenomanian. England
Xiphactinus mantelli Newton, 1877	Cenomanian-Campanian. Europe
Xiphactinus vetus (Leidy, 1870)	Campanian-Maastrichtian. USA

part of the posterior preurals and urals; the pectoral and pelvic fins lack saber-like rays; and, if it is present, the ethmopalatine is not identifiable because a huge antorbital bone covers the base of the ethmoid skull region (Hacker and Shimada, 2021, figures 3–5). Additionally, *Bradackichthys* shows multiple pores in the lateral surface of the vertebrae, which differ from the presence of two large oval longitudinal cavities separated by a ridge present in the "true" ichthyodectiforms.

The inclusion of *Jinjuichthys* and *Mesoclupea* within the order Ichthyodectiformes is also refutable. The case of *Jinjuichthys* is like that of *Bardackichthys*; the available specimens show uroneurals in dorsal position, likely lack the ethmopalatine, have no saber-like rays in the pelvic and pectoral fins, and three or four longitudinal cavities ornament the lateral faces of the vertebrae (Kim et al., 2014, figures 3–6). In contrast, the case of *Mesoclupea* differs notably. Ping and Yen (1933) erected this genus with two nominal species, thinking that

they were primitive herrings attributable to the family Clupeidae. Later, Chang (1963) synonymized these species and put *Mesoclupea showshangensis* into the family Chirocentridae (in which the genus type is the wolf-herring *Chirocentrus* Forsskål, 1775) together with other genera now grouped into the order Ichthyodectiformes (e.g., *Thrissops* and *Ichthyodectes*). Finally, Yabumoto (1994) erected the family Chuhsiungichthiidae into the order Ichthyodectiformes, including *Mesoclupea* and three species of the genus *Chuhsiungichthys* Lew, 1974 (*C. tsanglingensis* Lew, 1974 from China, plus his Japanese species *C. yanagidai* and *C. japonicus*). At first glance, these Asian fishes share the general body shape with the short-bodied ichthyodectiforms (i.e., *Chiromystus* Cope, 1885 and *Africathrissops* Taverne, 2010), but a closer view of the osteological data and images published by these authors (Ping and Yen, 1933; Chang, 1963; Yabumoto, 1994) do not allow their addition to Ichthyodectiformes. Against the "true" ichthyodectiforms, in chuhsiungichthiids, the uronerals cover only part of the dorsal surface of the ural and preural centra, the pelvic and pectoral rays also lack the saber-shaped rays, and the presence of the ethmopalatine is questionable. Chuhsiungichthiids also have the mouth open anteriorly, comparatively short jaw bones, and the premaxilla has an ascending anterior process, which are features not present in any "true" ichthyodectiforms.

Phylogenetic Results

Figure 15 contrasts the two phylogenetic hypotheses of Ichthyodectiformes. As noted in the "Materials and Methods" section, analysis 1 includes all the taxa considered in the data matrix, and analysis 2 excludes *Bardackichthys, Jinjuichthys,* and *Mesoclupea* (see Table S3 in Appendix 1). The tree obtained with all the taxa is a Strict Consensus Tree (SCT) generated from the 1,269 equally most parsimonious trees (MPT) in analysis 1, in which all characters are informative and have the following parameters: Tree length = 255 steps, Consistency Index (CI) = 0.4157, Homoplasy Index (HI) = 0.5843, CI Excluding Uninformative Characters (CIEUC) = 0.4016, HI excluding uninformative characters (HIEUC) = 0.5962, Retention Index (RI) = 0.5962, and Rescaled Consistency Index (RCI) = 0.2478. Otherwise, the resulting tree of the phylogenetic analysis 2 represents an SCT of 276 equal MPTs of 230 steps, in which the characters 21, 33, 47, 54, and 56 are uninformative, CI = 0.4565, HI = 0.5435, CIEUC = 0.4444, HIEUC = 0.5556, RI = 0.6082, and RCI = 0.2776.

Overall, the hypotheses 1 and 2 have similar topologies (Figure 16) and resemble those recently published by other authors (i.e., Berrell et al., 2014; Yabumoto et al., 2018; Cavin and Berrell, 2019; Baños-Rodríguez et al., 2020; Hacker and Shimada, 2021). In these, the Jurassic genera — *Occithrissops* Schaeffer, Patterson, 1984; *Allothrissops* Nybelin, 1964; and *Thrissops* — represent the basal taxa, and all Cretaceous ichthyodectiforms occupy a more derived position (node E) (*Jinjuichthys* and *Mesoclupea* are part of these basal forms in analysis 1). Although phylogenetic analysis 2 does not obtain the clade traditionally known as Saurodontidae (Node L) and only shows a minimal increase in the IC value compared with analysis 1 (0.4157 versus 0.4565), its topology is more consistent because it includes eight of the 15 clades with Bremer and Bootstrap values of greater than two and 52 (versus five of 16 obtained in hypothesis 1).

Table S3 in Appendix 1 shows a complete description of hypotheses 1 and 2. Only the unambiguous supporting characters of the nodes that include *Amakusaichthys benammii* sp. nov. are described below. According to both resulting hypotheses (Figure 16, Node A), four unambiguous synapomorphies support the monophyly of the Ichthyodectiformes [teeth aligned in a single alveolar row in both jaws (ch. 21-1); the articular bone forms part of the facet for the quadrate (ch. 33-2); the coracoids are broad and meet to each other middle-ventrally (ch. 47-1); and the first anal and dorsal pterygiophores elongated, arranged in clusters that extend into the interhemal spaces (ch. 54-1)].

In the present hypotheses, *Allothrissops mesogaster* (Agassiz, 1833) represents the basal taxon and the sister of an unnamed group (Figure 16, Node B). Two unambiguous synapomorphies support this group [the intercalar bone is large, forms part of the hyomandibular facet of the skull, and encloses a canal for the jugular vein (ch. 6-1); the mouth is directed upward (ch. 35-1)]. An additional ambiguous character is defined by the optimization acctran in both hypotheses [the epineurals are elongated (ch. 56-1)]. Both hypotheses share four unambiguous homoplasies supporting this unnamed "Ichthyodectiformes *minus Allothrissops"* clade [the parasphenoid is toothless (ch.9-1); the ethmopalatine is large and has no membranous outgrowth (ch. 13-2); the premaxilla is poorly attached to maxilla (ch. 18-1); and the parietal branch of the supraorbital sensory canal present as an anterior pit line only (ch. 41-1)]. The

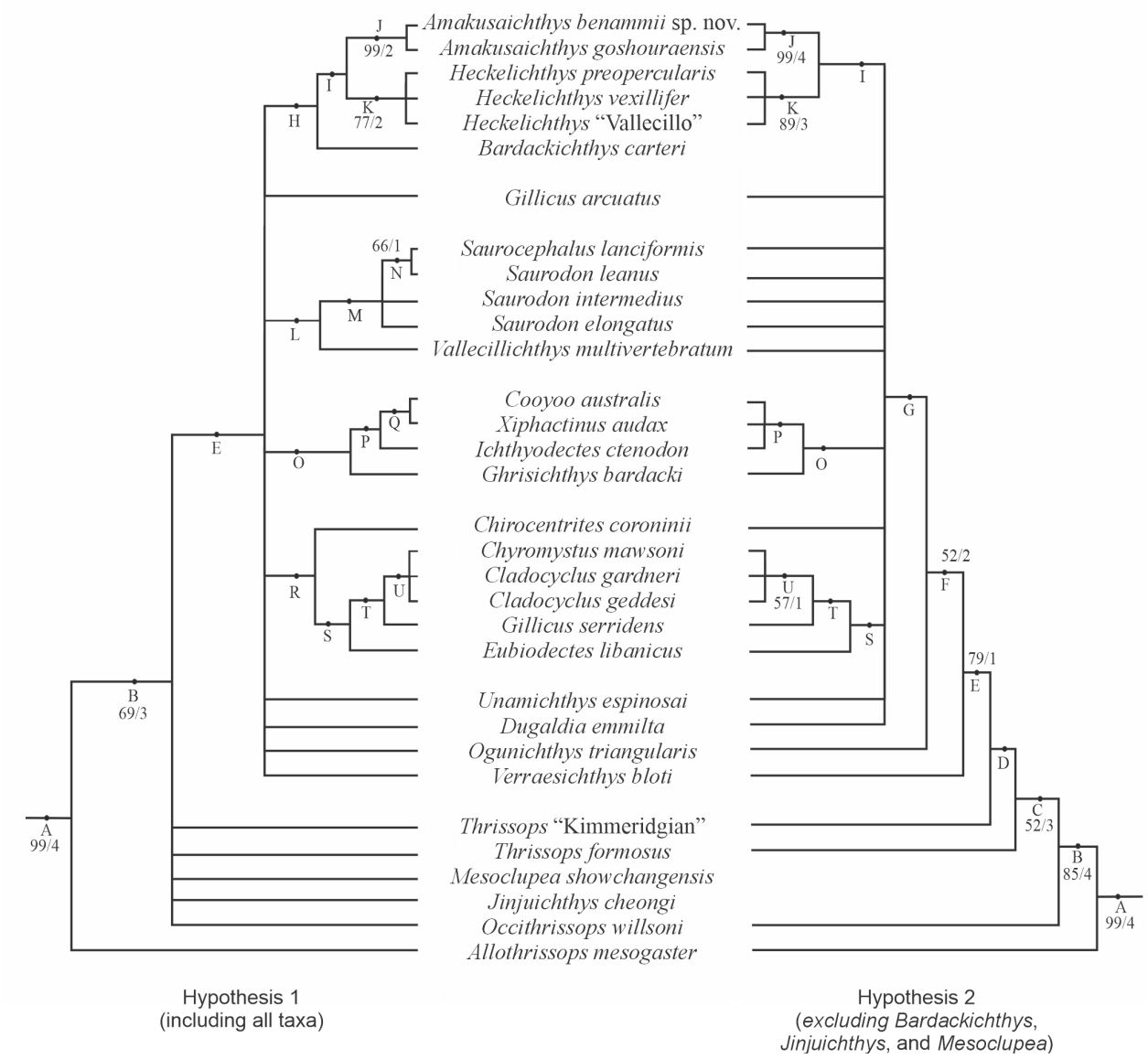

FIGURE 16. Phylogenetic hypotheses of the Ichthyodectiformes including *Amakusaichthys benammii* sp. nov., showing the trees generated through 50% consensus and strict consensus criteria (see Appendix 1 for a complete description). The values expressed as X/Y in nodes B, R, S, and V show the bootstrap (above) and Bremmer (below) values obtained in the present study; in other nodes, these values are lower than 50% and 1, respectively.

presence of a parasphenoid bone with a pronounced angle beneath the posterior margin of the orbit (ch.10-1) is an additional ambiguous supporting homoplasy of this group in hypothesis 1.

Next, hypothesis 2 shows a group with the species of *Thrissops* and all the Cretaceous ichthyodectiforms (Figure 16, Node C). Three unambiguous characters support this clade, including a synapomorphy [(presence of epioccipital crests (ch. 1-1)] and two homoplasies [the supraoccipital crest is large (ch. 2-2), and the basal sclerotic bone with serrated margins is present (ch. 16)]. Also, only hypothesis 2 shows a group that includes *Thrissops* "Kimeridgian" (Cavin et al., 2013) plus Cretaceous ichthyodectiforms (Figure 16, Node D) that is supported weakly by a single unambiguous homoplasy [the presence of symphyseal teeth (ch. 25-1)].

Although Cretaceous ichthyodectiforms form a natural group in both hypotheses obtained in this work (Figure 16, Node E), this group is supported weakly by three unambiguous homoplasies [the ethmopalatine bone is large and has membranous outgrowings with membranous outgrowths sepa-

rating and suturing with the rostrodermethmoid and lateroethmoid (ch. 13-3); the premaxilla is attached firmly to maxilla (ch. 18-2); and the lateral surfaces of vertebrae have two deep longitudinal grooves separated by a middle ridge (ch. 59-1)]. In hypothesis 2, an additional unambiguous homoplasy supports this group [the mandible-inferior quadratus joint is on the anterior margin of the forward orbit (ch. 34-1)].

In hypothesis 2 of this work, the Cretaceous ichthyodectiforms are subdivided into three subgroups showing a comb-like order. The first excludes *Verraesichthys* Taverne, 2010 (Figure 16, Node F). It is weakly defined by four unambiguous homoplasies [the supraoccipital crest becomes large and exceeds the occipital region (ch. 2-1), the maxilla is machete-shaped (ch. 20-0), dentary teeth have irregular sizes (ch. 26-1), the first three or four extend anteroventrally, covering the lateral surface of the urals and posterior preural centra (ch. 64-1)]. The second one excludes *Verraesichthys* and *Ogunichthys* (Figure 16, Node G) and is supported weakly by a single unambiguous homoplasy [dorsally, the rostrodermethmoid has a slight constriction behind the initial extension (ch. 14-1)]. Finally, the third group is a polytomy of nine species representing six genera (*Chirocentrites* Heckel, 1849; *Dugaldia* Cavin and Berrell, 2019; Eubiodectes Hay, 1903; *Gillicus* Hay, 1898; *Saurocephalus, Saurodon* Hays, 1830; *Unamichthys* Alvarado-Ortega, 2004, and *Vallecillichthys* Blanco and Cavin, 2003) plus three clades (Figure 16, Nodes I, O, and S).

In hypothesis 1, *Amakusaichthys benammii* sp. nov. is included in the already named Family Bardackichthyidae, here scarcely supported in two unambiguous homoplasies [the caudal fin has a ventral lobe at least 1.4 times longer than the dorsal lobe (ch. 58-1), and the hemal arches fuse to the respective caudal centra (ch. 60-1)]. In contrast, hypothesis 2 excludes *Bardachichthys* for the reasons already discussed in the previous section of this work.

In both hypotheses of this work, the species of *Amakusaichthys* and *Heckelichthys* form a natural group (Figure 16, Nodes I) supported on two unambiguous homoplasies [the lower jaw-quadrate articulation is in front of the orbit and below the lateroethmoid (ch. 34-2), and the dorsal fin is shorter than the anal fin, its anterior end opposes the anterior lobe of the anal fin (both arise far in the back of the trunk) (ch. 53-4)]. Additionally, hypothesis 1 shows a single synapomorphy of this group [the length of the preopercular horizontal limb is larger than the height of the preopercular vertical limb (ch. 73-1)], and hypothesis 2 displays two other unambiguous homoplasies [the articular and alveolar parts of the maxilla are equally high, and its ventral and dorsal margins are parallel (ch. 20-1); and the anterior ceratohyal has no foramen (ch. 40-0)].

This research demonstrates the naturalness of *Amakusaichthys* (Figure 16, Nodes J). Its supporting characters in both hypotheses include two common unambiguous homoplasy [presence of replacement tooth alveoli (ch. 28-1), and the number of total vertebrae ranges between 76 and 85 (ch. 69-1)]. Additional supporting characters of this clade differ between these hypotheses. On the one side, hypothesis 1 also shows three unambiguous synapomorphies [the hypural 2 is triangular and larger than hypural 1 (ch. 75-1), hypural 2 has a folded ridge in the anterior part of its dorsal edge (ch. 76-1), and the neural spines of preural centra has a saddle-shaped process (ch. 77-1)]. On the other side, hypothesis 2 shows another unambiguous homoplasy [in the pectoral fin, the first ray is 1.5 times the breadth of the second (ch. 48-1)].

Osteological Remarks

Recent paleontological studies have significantly expanded the knowledge of the taxonomic diversity of Ichthyodectiformes. Without excluding some questionable species, today, the order involves 75 species representing 44 genera (Table 2); however, most of their relationships are still unclear. Undertaking a comparative osteological exercise in this scenario looks hard; nevertheless, specimens of the type series of *Amakusaichthys benammii* sp. nov. exhibit enough osteological features to recognize it as an undisputed member of the order Ichthyodectiformes and the suborder Ichthyodectoidei sensu Patterson and Rosen (1977).

This new species has the non-exclusive body features of Ichthyodectiformes previously documented by now classical researchers of the order (Bardack, 1965; Bardack and Sprinkle, 1969; Patterson and Rosen, 1977; Schaeffer and Patterson, 1984; Maisey, 1991), such as an elongated and uniformly high body with a relatively small head, jaws with a single tooth row, the deeply bifurcated caudal fin, and unpaired fins placed far back on the trunk and opposed to each other (i.e., Figures 2, 7). In addition, the new species has the most outstanding diagnostic features of this fish order, a pair of ethmopalatine bones forming the floor of the nasal capsule and the broad or saber-like shape of

the first rays in the pectoral and pelvic fins (Figures 5–6).

The review of the description of the only specimen of *Bardaichthys carteri* so far known (Hacker and Shimada, 2021) allows us to challenge its belonging to the order Ichthyodectiformes and point out the unnatural condition of the Family Bardackichthyidae (which also includes *Heckelichthys* and *Amakusaichthys*). Despite such observations, the reconsideration or definitive expulsion of *Bardaichthys, Jinjuichthys,* and *Mesoclupea*, as part of this order, must still pass through the task of reassessing the osteological evidence exhibited by the available fossil materials. For now, and given that both phylogenetic hypotheses obtained in this work, one including and the other excluding these three genera (Figure 16), show the sister-group relationship of *Heckelichthys* and *Amakusaichthys*, this natural group is named family Heckelichthyidae. The subsequent possible reincorporation of *Bardackichthys* as a "true" ichthyodectiform would only cause the re-ranking of the clade *Heckelichthys-Amakusaichthys* to subfamily level.

Among ichthyodectiforms, *Heckelichthys* and *Amakusaichthys* share the following unique combination of features. The supraoccipital crest is large but shallow and does not project beyond the base of the skull (Figures 5–7); the teeth in both jaws are evenly small or absent (Figure 8); the origin of the unpaired fins oppose each other (Figure 4); the preopercle exhibits a short horizontal limb; the mandibular articulation is below and in front of the orbit (Figure 9); and the caudal fin has the ventral lobe at least 1.4 times longer than the dorsal lobe (Figure 2). On the contrary, in other ichthyodectiforms, the crest is small or large, noticeably higher, and can extend backward beyond the limit of the base of the skull; the dorsal fin arises behind the anterior lobe of the anal fin; the preopercle has a vertical limb longer than the horizontal limb one; the mandibular articulation is below or behind the posterior half of the orbit; and the length of the caudal ventral lobe is no more than 1.3 times the caudal dorsal lobe.

Since the fossil of *Amakusaichthys goshouraensis* only includes the impressions of incomplete specimens, the study of its osteology is limited. Fortunately, the type series of *A. benammii* sp. nov. includes well-preserved and complete specimens that allow access to fine osteological details after being prepared by different methods. Thus, the information from these Mexican fossils amends the generic diagnosis and reveals unusual features not previously observed in other ichthyodectiforms. Both *Amakusaichthys* species share the long-nose appearance of the head because the ethmoid region of the skull is noticeably longer than the orbit and its postorbital region. In addition, these have a caudal skeleton reinforced by the anterior elongation of the caudal rays; the hypural 2 is triangular, the more prominent in the series, and expanded posteriorly, with a dorsal folded corner ridge in its anterior two-thirds, pierced by three large pores aligned longitudinally and roofing a cavity that allocates the anterior tips of some rays of the ventral caudal fin lobe. Although not included in the original description of *A. goshouraensis* (Yabumoto et al., 2018, figures 5–6), these species also share the presence of dorsoanterior saddle-shaped processes in the neural arches of preurals 2–7, the parhypural and hypurals 1–2 have enlarged articular heads expanded laterally, and the hypural 3 is shorter than the hypural 2 (Figures 9, 12, 13).

Noticeably, the Late Cretaceous Italian ichthyodectiforms *Garganoichthys alfonsoi* Taverne, 2009, and *Altamuraichthys meleleoi* Taverne, 2016, share at least part of the *Amakusaichthys* features listed above; nevertheless, their possible inclusion into a family Heckelichthyidae must wait for an accurate analysis of the available specimens. Overall, the features of the body, head, and unpaired fins of the single specimen of *Altamuraichthys* resemble *Amakusaichthys*; its imperfect caudal skeleton shows traces of the saddle-shaped processes in the neural arches of posterior preural centra. In the incomplete and single specimen available of *Garganoichthys,* the origins of both unpaired fins oppose each other, and the hypural 2 (described initially as hypural 1 by Taverne (2009, figure 5) has three small perforations resembling those of *A. benammii*.

Finally, the diagnosis of *Amakusaichthys benammii* sp. nov. exhibits numerous features that support its specific identity and fully differentiate it from *A. goshouraensis.* It is noticeable that some of these features have not been observed in other ichthyodectiforms, suggesting that this fish is highly specialized. Among these, the most outstanding features are the frontoparietal fontanelle, the intense ornamentation in the dorsal surface of the dorsal skull bones, the anterior position of the ethmopalatine ahead the nasal capsule and with a dorsal extension bordering the anterior margin of this capsule, the ventral processes with ending plates (the anterior hard-shaped and posterior arrow-shaped) the present behind the parasphenoid basipterygoid process (unfortunately the prob-

able masticatory function of these plates are unsure because pharyngeal teeth have not yet observed in *A. benammii*); the oval opercle exposing the hyomandibular facet at the middle height of its curved anterior edge; the dorsal palatine notch in the maxilla; the hypural 3 shortened and with a small unpierced folded corner ridge turned upward.

Both *Amakusaichthys* species differ in two features, which may be controversial in the specimens of *A. goshouraensis*. As observed in this work, *A. benammii* sp. nov. has autogenous hemal arches and dentary teeth homogeneously small (Figures 7, 9, 12, 13). In contrast, in *A. goshouraensis,* such arches are interpreted as fused to their respective preural centrum, and the dentary teeth are reported as irregularly sized (Yabumoto et al., 2018, appendix 2).

CONCLUSIONS

The long-nose ichthyodectiform specimens recovered in the Campanian shallow marine marl deposits of the Tzmol Quarry in Chiapas, southeastern Mexico, represent a new species, here named *Amakusaichthys benammii*. These fossils display significant osteological features supporting their recognition as a new species of Ichthyodecyiformes, suborder Ichthyodectoidei, and genus *Amakusaichthys.* This second species of *Amakusaichthys* is also the youngest and best represented in the fossil record.

Including *Amakusaichthys benammii* sp. nov. in a comparative exercise and a phylogenetic analysis shows that *Amakusaichthys* and *Heckelichthys* are closely related. Therefore, these are placed here within the new family of Heckelichthyidae. Although these two genera and *Bardackichthys* were previously part of the family Bardackichthyidae, the relevance of this family and the position of *Bardackichthys* in the order Ichthyodectiformes are questionable because it seems does not have the most notable diagnostic features of the order Ichthyodectiformes.

On the one side, Heckelichthyidae involves fishes with peculiar features in the jaws (the teeth are absent or small conical and evenly sized and spaced; the lower jaw articulation is in front of the orbit) and fins (the origins of the anal and dorsal fins are opposed far in the back of the trunk, and the ventral caudal lobe is distinctively longer). On the other side, *Amakusaichthys* diagnosis includes a unique feature that reinforces the caudal skeleton (e.g., caudal rays elongated anteriorly, the hypural 1 is comparatively tiny and spatuliform; the parhypural and hypural 1 and 2 have broad articular heads; the hypural 2 is triangular, hypertrophied, and has a prominent and pierced dorsal folded corner ridge bent dorsally). Part of these diagnostic features seem to be present in *Garganoichthys* and *Altamuraichthys* (Taverne, 2009, 2016); however, a critical review and redescription of these fossils must precede their inclusion into the family Heckelichthyidae.

ACKNOWLEDGMENTS

I owe the institutions and people who made this research possible. I am grateful to local Tzimol Quarry workers and the students who helped me during the field seasons. UNAM provided financial support for this research through the grant DGAPA-PAPIIT IN115223.

REFERENCES

Adkins, W.S. 1930. New rudistids from the Texas and Mexican Cretaceous. The University of Texas Bulletin, Contribution to Geology, 3001:77–99.

Agassiz, L. 1833. Recherches sur les poisons fossils, volume 1 (preface dated in1833), Neuchâtel, Suisse.

Agassiz, L. 1841. On the fossil fishes found by Mr. Gardner in the Province of Ceará, in the north of Brazil. Edinburgh New Philosophical Journal, Edinburgh, 30:82–84.

Agassiz, L. 1844. Recherches sur les poisons fossils, Volume 2 (preface dated in1843), Neuchâtel, Suisse.

Alvarado-Ortega, J. 1998. Ichthyodectiformes mexicanos: un análisis de su diversidad, p.109–119. In Carranza-Castañeda, O. and Córdoba-Méndez, D.A. (eds.), Avances en investigación – Paleontología de Vertebrados. Instituto de Investigaciones en Ciencias de la Tierra, Universidad Autónoma del Estado de Hidalgo, Pachuca, México.

Alvarado-Ortega, J. 2004. Description and relationships of a new ichthyodectiform fish from the Tlayúa Formation (Early Cretaceous: Albian), Puebla, Mexico. Journal of Vertebrate Paleontology, 24:802–813. https://doi.org/10.1671/0272-4634(2004)024[0802:DAROAN]2.0.CO;2

Alvarado-Ortega, J. 2005. Sistemática de los peces Ichthyodectiformes de la cantera Tlayúa, Puebla, México. Unpublished PhD Thesis, Universidad Nacional Autónoma de México, Distrito Federal, México.

Alvarado-Ortega, J., Ovalles-Damián, E., and Blanco-Piñón, A. 2009. The fossil fishes from the Sierra Madre Formation, Ocozocoautla, Chiapas, Southern Mexico. Palaeontologia Electronica, 12.2.4A:1–22. https://palaeo-electronica.org/2009_2/168/index.html

Alvarado-Ortega, J. and Porras-Múzquiz, H.G. 2009. Acerca de la presencia de *Gillicus arcuatus* (Cope, 1875) (Pisces, Ichthyodectiformes†) en México. Boletín de la Sociedad Geológica Mexicana, 61:215–224.

Alvarado-Ortega, J. and Brito, P.M. 2010. A new ichthyodectiform fish (Teleostei) from the Early Cretaceous Marizal Formation, Northeast Brazil. Palaeontology, 53:297–306. https://doi.org/10.1111/j.1475-4983.2010.00935.x

Alvarado-Ortega, J., Cantalice Severiano, K.M., Pacheco Ordaz, S., Díaz-Cruz, J.A., and Carranza Becerra, B. 2019. Las Canteras Tzimol nuevos yacimientos fosilíferos con peces del Campaniano en Chiapas. Libro de Resúmenes, XXIV Congreso Nacional de Zoología, Monterrey, in press.

Alvarado-Ortega, J., Cantalice, K.M., Martínez-Melo, A., García-Barrera, P., Than-Marchese, B.A., Barrientos-Lara, J.I., and Díaz-Cruz, J.A. 2020. Tzimol, a Campanian marine paleontological site of the Angostura Formation near Comitán, Chiapas, southeastern Mexico. Cretaceous Research, 107:104279. https://doi.org/10.1016/j.cretres.2019.104279

Alvarado-Ortega, J. and Porras-Muzquiz, H.G. 2022. On the presence of *Xiphactinus* (Teleostei, Ichthyodectiformes) in the Coniacian-Campanian marine deposits of the Piedritas site, Coahuila, northern Mexico. Revista Mexicana de Ciencias Geologicas, 39:142–150. https://doi.org/10.22201/cgeo.20072902e.2022.2.1684

Arbour, V.M. and Currie, P.J. 2011. An istiodactylid pterosaur from the Upper Cretaceous Nanaimo Group, Hornby Island, British Columbia, Canada. Canadian Journal of Earth Sciences, 48:63–69.

Arratia, G. 2000. Remarkable teleostean fishes from the Late Jurassic of southern Germany and their phylogenetic relationships. Mitteilungen aus dem Museum für Naturkunde in Berlin, Geowissenschaften Reihe, 3:137–179. https://doi.org/10.1002/mmng.20000030108

Arratia, G., Scasso, R.A., and Kiessling, W. 2004. Late Jurassic fishes from Longing Gap, Antarctic Peninsula. Journal of Vertebrate Paleontology, 24:41–55. https://doi.org/10.1671/1952-4

Baños-Rodríguez, R.E. 2018. Taxonomía y Sistemática de los peces Ichthyodectiformes (Teleostei) de la Cantera Muhi (Albiano-Cenomaniano) de Zimapán, Hidalgo, México. Unpublished Master's thesis. Universidad Autónoma del Estado de Hidalgo, México.

Baños-Rodríguez, R.E., González-Rodríguez, K.A., Wilson, M.V., and González-Martínez J.A. 2020. A new species of *Heckelichthys* from the Muhi Quarry (Albian–Cenomanian) of central Mexico. Cretaceous Research, 110:104415. https://doi.org/10.1016/j.cretres.2020.104415

Bardack, D. 1965. Anatomy and evolution of chirocentrid fishes. The University of Kansas paleontological contributions: Vertebrata, 10:1–88.

Bardack, D. and Sprinkle, G. 1969. Morphology and relationships of saurocephalid fishes. Fieldiana Geology, 16:297–340. https://doi.org/10.5962/bhl.title.5210

Bassani, F. 1879. Vorläufige Mitteilungen über die Fischfauna der Insel Lesina. Verhandlungen der Kaiserlich-Königlichen Geologischen Reichsanstalt, 1879:162–170.

Berrell, R.W., Alvarado-Ortega, J., Yabumoto, Y., and Salisbury, S.W. 2014. The first record of the ichthyodectiform fish *Cladocyclus* from eastern Gondwana: a new species from the Lower Cretaceous of Queensland, Australia. Acta Palaeontologica Polonica, 59:903–920. https://doi.org/10.4202/app.2012.0019

Blanco-Piñón, A. and Alvarado-Ortega, J. 2007. Review of *Vallecillichthys multivertebratum* (Teleostei: Ichthyodectiformes), a Late Cretaceous (early Turonian) bulldog fish from northeastern Mexico. Revista Mexicana de Ciencias Geológicas, 24:450–466.

Blanco, A. and Cavin, L. 2003. New Teleostei from the Agua Nueva Formation (Turonian), Vallecillo (NE Mexico). Comptes Rendus Palevol, 2:299–306. https://doi.org/10.1016/S1631-0683(03)00064-2

Blainville, H.M.D. 1818. Sur les ichthyolites ou les poissons fossiles, in Nouveau Dictionnaire d'Histoire Naturelle, appliquée aux arts, Tome XXVII. D´Abel Lanoe, Paris.

Blot, J. 1987. L'Ordre des Pycnodontiformes. Museo Civico di Storia Naturale di Verona, Studi e ricerche sui giacimenti terziari di Bolca, 5:1–211.

Carranza-Becerra, B., Cantalice, K.M., and Alvarado-Ortega, J. 2023. Nuevos registros de Acanthomorphos (Actinopterygii, Teleostei) del Campaniano (Cretácico Superior) de la cantera Tzimol (Chiapas, México). Memorias, XVII Congreso Nacional de Ictiología & IX Simposio Latinoamericano de Ictiología, La Paz, p.164.

Cavin, L. 1997. Nouveaux Teleostei du gisement Turonien inférieur de Goulmima (Maroc). Comptes Rendus de l'Académie des Sciences, 325:719–724. https://doi.org/10.1016/S1251-8050(97)89116-1

Cavin, L., Forey, P.L., and Giersch, S. 2013. Osteology of *Eubiodectes libanicus* (Pictet & Humbert, 1866) and some other ichthyodectiformes (Teleostei): phylogenetic implications. Journal of Systematic Paleontology, 11:115–177. https://doi.org/10.1080/14772019.2012.691559

Cavin, L. and Berrell, R.W. 2019. Revision of *Dugaldia emmilta* (Teleostei, Ichthyodectiformes) from the Toolebuc Formation, Albian of Australia, with comments on the jaw mechanics. Journal of Vertebrate Paleontology, 39:e1576049. https://doi.org/10.1080/02724634.2019.1576049

Chang, M.-M. 1963. New materials of *Mesoclupea* from southeastern China and on the systematic position of the genus. Vertebrata PalAsiatica, 7:105–122.

Cope, E.D. 1870. On the Saurodontidae. American Philosophical Society, Proceedings, 11:529–538.

Cope, E.D. 1871. On two extinct forms of Physostomi of the Neotropical region. Proceedings of the American Philosophical Society, 12:52–55.

Cope, E.D. 1875. The vertebrata of the Cretaceous formations of the west: Washington, DC, United States Geological Survey of the Territories, Government Printing Office, Report, 2:281–293.

Cope, E.D. 1885. A contribution to Vertebrate Paleontology of Brazil. Proceedings of the American Philosophical Society, 23:1–21.

Costa, O.G. 1865. Nuove osservazioni e scoperte intorno ai fossili della calcarea ad ittioliti di Pietraroja. Atti dell'Accademia delle Scienze Fisiche e Matematiche di Napoli, 1(22):1–12.

Davies, W. 1878. On the nomenclature of *Saurocephalus lanciformis* of the British Cretaceous deposits: with description of a new species (*S. woodwardii*). Geological Magazine, 15:254–261. https://doi.org/10.1017/S0016756800150289

Díaz-Cruz, J.A., Alvarado-Ortega, J., and Cantalice, K.M. 2022. *Apuliadercetis gonzalezae* sp. nov., a North American Campanian dercetid fish (Teleostei, Aulopiformes) from Tzimol, Chiapas, Mexico. Cretaceous Research, 130:105060. https://doi.org/10.1016/j.cretres.2021.105060

Dixon, F. 1850. The geology and fossils of the Tertiary and Cretaceous formations of Sussex. Longman, Brown, Green, and Longmans, London.

Egerton, P.G. 1845. On some new species of fossil fish from the Oxfordc1ayat Christian Malford. Quarterly Journal of the Geological Society of London, 1:229–232. https://doi.org/10.1144/GSL.JGS.1845.001.01.61

Felix, J. 1891. Versteinerungenaus der mexicanischen Jura und Kreide Formation. Palaeontographica, 37:140–194.

Forey, P.L. and Cavin, L. 2007. A New Species of †*Cladocyclus* (Teleostei: Ichthyodectiformes) from the Cenomanian of Morocco. Palaeontologia Electronica, 10.3.12A:1–10. https://palaeo-electronica.org/2007_3/133/index.html

Forsskål, P.S. 1775. Descriptiones animalium avium, amphibiorum, piscium, insectorum, vermium; quae in itinere orientali observavit. Post mortem auctoris edidit Carsten Niebuhr. Ex officina Mölleri, aulae typographi, Hauniae. https://doi.org/10.5962/bhl.title.2154

González-Rodríguez, K.A., Espinosa-Arrubarrena, L., and González-Barba, G. 2013. An overview of the Mexican fossil fish record, p. 9–24. In Arratia, G., Schultze, H.-P., and Wilson, M.V.H. (eds.), Mesozoic Fishes 5 – Global Diversity and Evolution and Phylogeny. Verlag Dr. Friedrich Pfeil, München, Germany.

Hacker, R.J.G. and Shimada, K. 2021. A new ichthyodectiform fish (Osteichthyes: Actinopterygii) from the Arlington Member (mid-Cenomanian) of the Upper Cretaceous Woodbine Formation in Texas, USA. Cretaceous Research, 12:104798. https://doi.org/10.1016/j.cretres.2021.104798

Harlan, R. 1824. On a new fossil genus of the order Enalio Sauri (of Conybeare). Journal of the Academy of Natural Sciences of Philadelphia, 3:331–337+1 pl. https://doi.org/10.1080/14786442408644630

Hay, O. P. 1898. Notes on species of *Ichthyodectes*, including the new species *I. cruentus*, and on the related and herein established genus *Gillicus*. American Journal of Science, 6:225–232.

Hay, O.P. 1903. On a collection of upper Cretaceous fishes from Mount Lebanon, Syria, with descriptions of four new genera and nineteen new species. Bulletin American Museum of Natural History, 19:395–451.

Hays, I. 1830. Description of a fragment of the head of a new fossil animal, discovered in a marl pit, near Moorestown, New Jersey: Transactions of the American Philosophical Society, Series 2, 3(18):471–477+ 16 pl.

Heckel, J.J. 1849. Abhandlung über eine neue fossile Fischgattung, *Chirocentrites*, und die ersten Über reste eines Siluroiden aus der Vorwelt. Akademie der Wissenschaften, Mathemattisch-Naturwissenchaftliche Klasse, Wien, 2:16–19.

Heckel, J.J. 1856. Beiträge zur Kenntniss der fossilen Fische Österreichs. Abhandlung II. Denkschriften der kaiserlichen Akademieder Wissenschaften, Mathematisch-Naturwissenschaftliche Klasse, Wien, 11:187–274.

Jaekel, O. 1909. Beitrage zur Geologie von Kamerun: X. Fischreste aus der Mamfe-Schiefern. Abhandlungen der Königlich-Preussischen Geologischen Landesanstalt, 62:392–398. https://doi.org/10.5962/bhl.title.67531

Jordan, D.S. 1910. Description of a collection of fossil fishes from the bituminous shales at Riaco Doce, State of Alagôas, Brazil. Annals of the Carnegie Museum, 7:23–34.

Kaddumi, H.F. 2009. Fossils of the Harrana Fauna and the Adjacent Areas. Eternal River Museum of Natural History, Amman, Jordan.

Kim, H.M., Chang, M.-M., Wu, F., and Kim, Y.H. 2014. A new ichthyodectiform (Pisces, Teleostei) from the Lower Cretaceous of South Korea and its paleobiogeographic implication. Cretaceous Research, 47:117–130. https://doi.org/10.1016/j.cretres.2013.11.007

Koslov, A. 1928. *Thrissops volgensis* sp. nov., from the Lower Volgian of the Government of Ulianovsk. Bulletins du Comité Géologique Leningrad, 47:573–580+1pl.

Leidy, J. 1857. Remarks on *Saurocephalus* and its allies. Transactions of the American Philosophical Society, 11:91–95+vi pls.

Leidy, J. 1870. Remarks on ichthyodorulites and on certain fossil Mammalia. Proceeding of Academy on Natural Science, Philadelphia, 22:12–13.

Lew, C.-C. 1974. A new Cretaceous Teleostei from Chuhsiung, Yunnan. Vertebrata PalAsiatica, 4(3):249–256.

Loomis, F.B. 1900. Die Anatomie und die Verwandtschaft der Ganoid- und Knochen-Fische aus der Kreide Formation von Kansas. USA. Palaeontographica, 46:213–286.

L-Recinos, M., Cantalice, K.M., Caballero-Viñas, C., and Alvarado-Ortega, J. 2023. A new Mesozoic teleost of the subfamily Albulinae (Albuliformes: Albulidae) highlights the proto-Gulf of Mexico in the early diversification of extant bonefishes. Journal of Systematic Palaeontology, 21:2223797. https://doi.org/10.1080/14772019.2023.2223797

Lupercio Espericueta, N. 2022. Paleoambientes de los depósitos fosilíferos del Campaniano de la Cantera Tzimol, Chiapas, México. Unpublished Master's thesis, Universidad Autónoma de San Luis Potosí, México.

Maddison, W.P. and Maddison, D.R. 2023. Mesquite: a modular system for evolutionary analysis. Version 3.81. http://www.mesquiteproject.org.
Maisey, J.G. 1991. *Cladocyclus* Agassiz, 1841, p. 190–207. In Maisey, J.G. (ed.), Santana Fossils, T.F.H. Publications Inc., New Jersey.
Maldonado-Koerdell, M. 1956. Peces fósiles de México III. Nota preliminar sobre peces del Turoniano superior de Xilitla, San Luis Potosí, México. Ciencia, 16:31–36.
Mayrinck, D. de, Ribeiro, A.C., Assine, M.L., and Spigolon, A.L.D. 2023. A New Genus and Species of †Cladocyclidae (Teleostei: †Ichthyodectiformes) from the Lower Cretaceous "Batateira Beds", Barbalha Formation, Araripe Basin: The First Vertebrate Record in a Still Poorly Explored Fossil Site. Diversity, 15(3):413. https://doi.org/10.3390/d15030413
Mkhitaryan, T.D. and Averinov, A.O. 2011. New material and phylogenetic position of *Aidachar paludalis* Nesov, 1981 (Actinopterygii, Ichthyodectiformes) from the Late Cretaceous of Uzbekistan. Proceedings of the Zoological Institute RAS, 315:181–192.
Müller, J. 1844. Über den Bau und die Grenzen der Ganoiden und über das natürliche System der Fische. Abhandlungen der Königlichen Akademie der Wissenschaften zu Berlin, 1846:119–216.
Nessov, L.A. 1981. Flying reptiles of Late Cretaceous of Kyzylkums. Paleontologicheskiy Zhurnal, 4:98–104.
Newton, E.T. 1877. On the remains of *Hypsodon, Phortheus* and *Ichthyodectes* from British Cretaceous strata, with description of a new species. Quarterly Journal of the Geological Society of London, 33:505–529+1pl.
Newton, E.T. 1878. Remarks on *Saurocephalus*, and on the species which have been referred to that genus. Quarterly Journal of the Geological Society of London, 34:786–796. https://doi.org/10.1144/GSL.JGS.1878.034.01-04.50
Nybelin, O. 1964. Versuch einer taxonomischen Revision der jurassischen Fisch- Gattung *Thrissops* Agassiz. Göteborgs Kungliga Vetenskaps-och Vitterhets- Samhälle Handlingar, Serie B, 9:351–432.
Patterson, C. and Rosen, D.E. 1977. Review of ichthyodectiform and other Mesozoic teleost fishes and the theory and practice of classifying fossils. Bulletin of the American Museum of Natural History, 158:83–172.
Pictet, F.J. 1858. Descriptions des fossils contenus dans terrain Néocomien des Voirons. Máter Paléontologie Suisse, 21:1–54+7 pls.
Pictet, F.J. and Humbert, A. 1866. Nouvelles recherches sur les poisons fossiles du Mont Liban. J-B. Baillère et fils-F. Savy, Géneva.
Ping, C. and Yen, T.C. 1933. Description of two new fossil fishes from Chekiang. Geological Society of China, Bulletin, 12:269–273+1 pl. https://doi.org/10.1111/j.1755-6724.1933.mp12001019.x
Ramaswami, L.S. 1955. Skeleton of the cyprinid fishes in relation to Phylogenetic studies: 7. The skull and Weberian Apparatus of Cyprininae. Acta Zoologica, 36:1–44. https://doi.org/10.1111/j.1463-6395.1955.tb00380.x
Regan, C.T. 1909. A revision of the fishes of the genus *Elops*. Annals and Magazine of Natural History, 3:37–40. https://doi.org/10.1080/00222930908692543
Romer, A.S. 1966. Vertebrate Paleontology, Third ed. University of Chicago Press, Chicago.
Sánchez-Montes de Oca, R. 1979. Geología petrolera de la Sierra de Chiapas. Boletín de la Asociación Mexicana de Geólogos Petroleros, 31:67–97.
Sauvage, H.-E. 1893. Note sur quelques poissons du calcaire bitumineux d'Orbagnoux (Ain). Bulletin trimestriel de la Société d'Histoire Naturelle d'Autun, 6:427–443.
Schaeffer, B. and Patterson, C. 1984. Jurassic fishes from the western United States, with comments on Jurassic fish distribution. American Museum Novitates, 2796:1–86.
Schultze, H.-P. 2008. Nomenclature and homologization of cranial bones in actinopterygians, p. 23–48. In Arratia, G., Schultze, H.-P., and Wilson, M.V.H. (eds.), Mesozoic Fishes 4. Verlag Dr. Friedrich Pfeil, München, Germany.
Silva-Santos, R. da. 1949. Sôbre alguns peixes fósseis do gênero *Chiromystus* da Ilha de Itaparica, Bahia. Notas Preliminares e Estudos, Divisão de Geologia e Mineralogia, Brazil, 50:1–12.

Stewart, J.D. 1999. A new genus of Saurodontidae (Teleostei: Ichthyodectiformes) from the Upper Cretaceous rocks of the Western Interior of North America, p. 335–360. In Arratia, G. and Schultze, H.-P. (eds.), Mesozoic Fishes 2 – Systematics and Fossil Record. Verlag Dr. Friedrich Pfeil, München, Germany.

Swofford, D.L. 2002. PAUP Phylogenetic analysis using parsimony and other methods Version 4.0a (Build 166). [Software]. Sinauer Associates, Sunderland, Massachusetts.

Taverne, L. 1977. Ostéologie et position systématiquedu genre *Thrissops* Agassiz, 1833 (sensu stricto) (Jurassique supérieur de l'Europe occidentale) au sein des Téléostéens primitifs. Geobios, 10:269–273. https://doi.org/10.1016/S0016-6995(77)80052-1

Taverne, L. 2008. Considerations about the Late Cretaceous genus *Chirocentrites* and erection of the new genus *Heckelichthys* (Teleostei, Ichthyodectiformes) – A new visit inside the ichthyodectid phylogeny. Bulletin de l'Institut royal des Sciences naturelles de Belgique, Sciences de la Terre, 78:209–228.

Taverne, L. 2009. Les poissons du Santonien (Crétacé supérieur) d'Apricena (Italie du Sud). 2°. *Garganoichthys decosmoi* gen. et sp. nov. (Teleostei, Ichthyodectiformes, Ichthyodectidae). Bollettino del Museo Civico di Storia Naturale di Verona, Geologia Paleontologia Preistoria, 33:27–39.

Taverne, L. 2010. Les Ichthyodectidae (Teleostei, Ichthyodectiformes) des schistes bitumineux de l'Aptien (Crétacé inférieur) de Guinée Équatoriale et du Gabon. Bulletin de l'Institut Royal des Sciences Naturalles de Belgique, Sciences de la Terre, 80:115–143.

Taverne, L. 2015. Les poissons crétacés de Nardò. 38°. *Capassoichthys alfonsoi* Gen. et sp. Nov. (Teleostei, Ichthyodectidae). Bollettino del Museo Civico di Storia Naturale di Verona, Geologia Paleontologia Preistoria, 39:35–46.

Taverne, L. 2016. Les poissons crétacés de Nardò. 39°. *Altamuraichthys meleleoi* gen. et sp. nov. (Teleostei, Ichthyodectiformes, Ichthyodectidae). Bollettino del Museo Civico di Storia Naturale di Verona, 40:3–20.

Taverne, L. and Bronzi, P. 1999. Les poissons Crétacés de Nardò. 9°. Note complementaire sur le saurodontinae (Teleostei, Ichthyodectiformes): *Saurodon elongatus*, sp. nov. Studi e Ricerche sui Giacimenti Terziari di Bolca, 8:105–116.

Taverne, L. and Capasso, L., 2018. Osteology and phylogenetic relationships of *Furloichthys bonarellii* gen. and sp. nov. (Teleostei, Ichthyodectidae), a tropical fish from the Upper Cretaceous of central Italy. Geo-Eco-Trop, 42:75–88.

Taverne, L. and Chanet, B. 2000. *Faugichthys loryi* n. gen., n. sp. (Teleostei, Ichthyodectiformes) de l'Albien terminal (Crétacé inférieur marin) du vallon de la Fauge (Isère, France) et considérations sur la phylogénie des Ichthyodectidae. Geodiversitas, 22:23–34.

Thiollére, V.J. 1854. Description des poisons fossils provenent des gisements coralliens du Jura dans le Bugey, Lyons. https://doi.org/10.3931/e-rara-41247

Toombs, H.A. and Rixon, A.E. 1959. The use of acids in the preparation of vertebrate fossils. Curator, 2:304–312. https://doi.org/10.1111/j.2151-6952.1959.tb00514.x

Villaseñor, A.B., Silva-Martínez, L.E., Olóriz, F., Blanco, A., and Alvarado-Ortega, J. 2006. Nuevo registro de peces Jurásicos en México. Memorias, X Congreso Nacional de Paleontología. Sociedad Mexicana de Paleontología, Ciudad de México, p. 137.

Wagner, A. 1863. Monographie der fossilen Fische aus den lithographischen Schiefern Bayern's. Zweite Abtheilung. Abhandlungen der mathematisch-naturwissenschaftlichen Abtheilung der königlichen bayerischen Akademie der Wissenschaften, 9(3):611–748.

Weiler, W. 1922. Die fischreste aus den bituminösen Schiefern von Ibando bei Bata (Spanisch Guinea). Paläontologische Zeitschrift, 5:148–160.

Woodward, A.S. 1894. On some fish remains of the genera *Portheus* and *Cladocyclus* from the Rolling Downs Formation of Queensland. Annals and Magazine of Natural History, Series 6, 14:444–447. https://doi.org/10.1080/00222939408677831

Woodward, A.S. 1895. Catalogue of the fossil fishes in the British Museum (Natural History), Volume 3. British Museum (Natural History), London. https://doi.org/10.5962/bhl.title.61854

Woodward, A.S. 1901. Catalogue of the fossil fishes in the British Museum (Natural History), Volume 4. British Museum (Natural History), London. https://doi.org/10.5962/bhl.title.61854

Woodward, A.S. 1919. The fossil fishes of the English Wealden and Purbeck formations. Monographs of the Palaeontographical Society, 3:105–148. https://doi.org/10.1017/CBO9781139680851

Yabumoto, Y. 1994. Early Cretaceous Freshwater fish fauna in Kyushu, Japan. Bulletin of the Kitakyushu Museum of Natural History, 13:107–254. https://doi.org/10.34522/bkmnh.13.0_107

Yabumoto, Y., Hirose, K., and Brito, P.M. 2018. A new ichthyodectiform fish, *Amakusaichthys goshouraensis* gen. et sp. nov., from the Upper Cretaceous (Santonian) Himenoura Group in Goshoura, Amakusa, Kumamoto, Japan. Historical Biology, 32:362–375. https://doi.org/10.1080/08912963.2018.1497022

APPENDIX 1.

Data used in the phylogenetic analysis of *Amakusaichthys benammii* sp. nov. (to download data see https://palaeo-electronica.org/content/2025/5295-a-long-nose-ichthyodectiform).

APPENDIX 2.

Nexus file of the phylogenetic analysis of *Amakusaichthys benammii* sp. nov. (to download data see https://palaeo-electronica.org/content/2025/5295-a-long-nose-ichthyodectiform).